Mathematical morphology in planetary surfaces characterization

Pedro Pina

IST – Instituto Superior Técnico

CERENA – Centro de Recursos Naturais e Ambiente

Lisboa, PORTUGAL

***Workshop Honouring Jean Serra*, Bangalore, India, October 25-26, 2010**

Sky is not the limit!

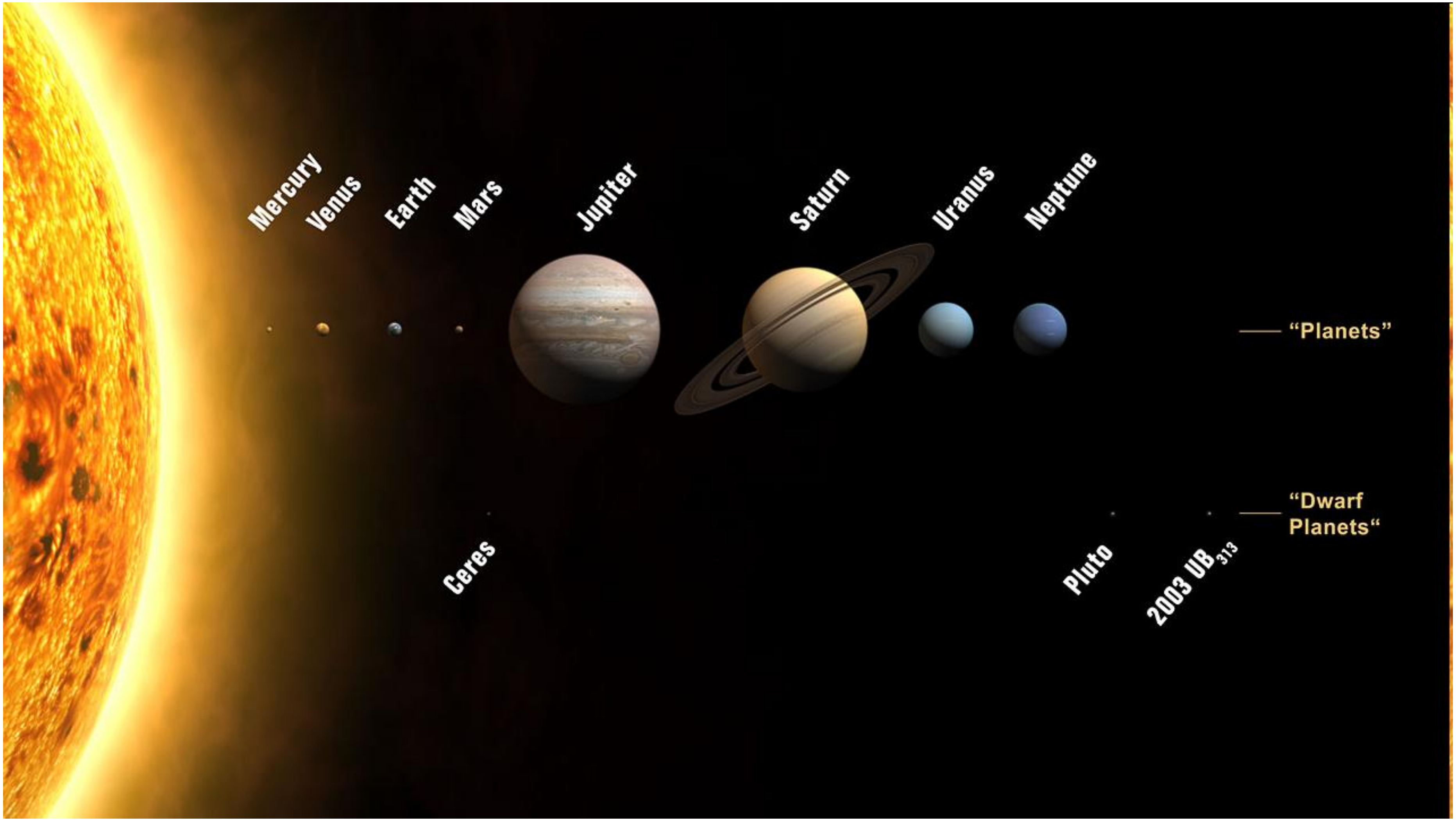

With many more moons!

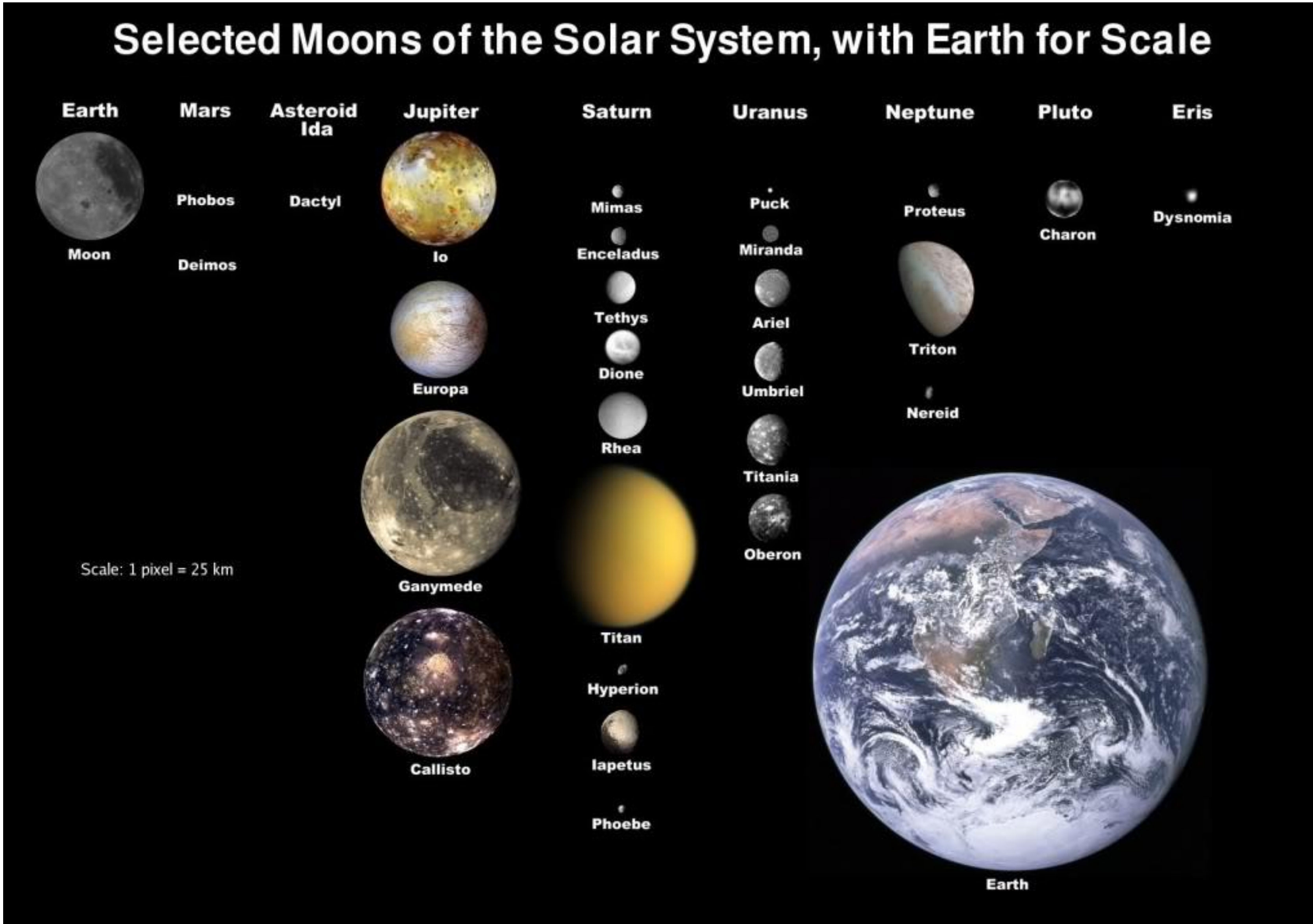

More than 50 years of planetary exploration

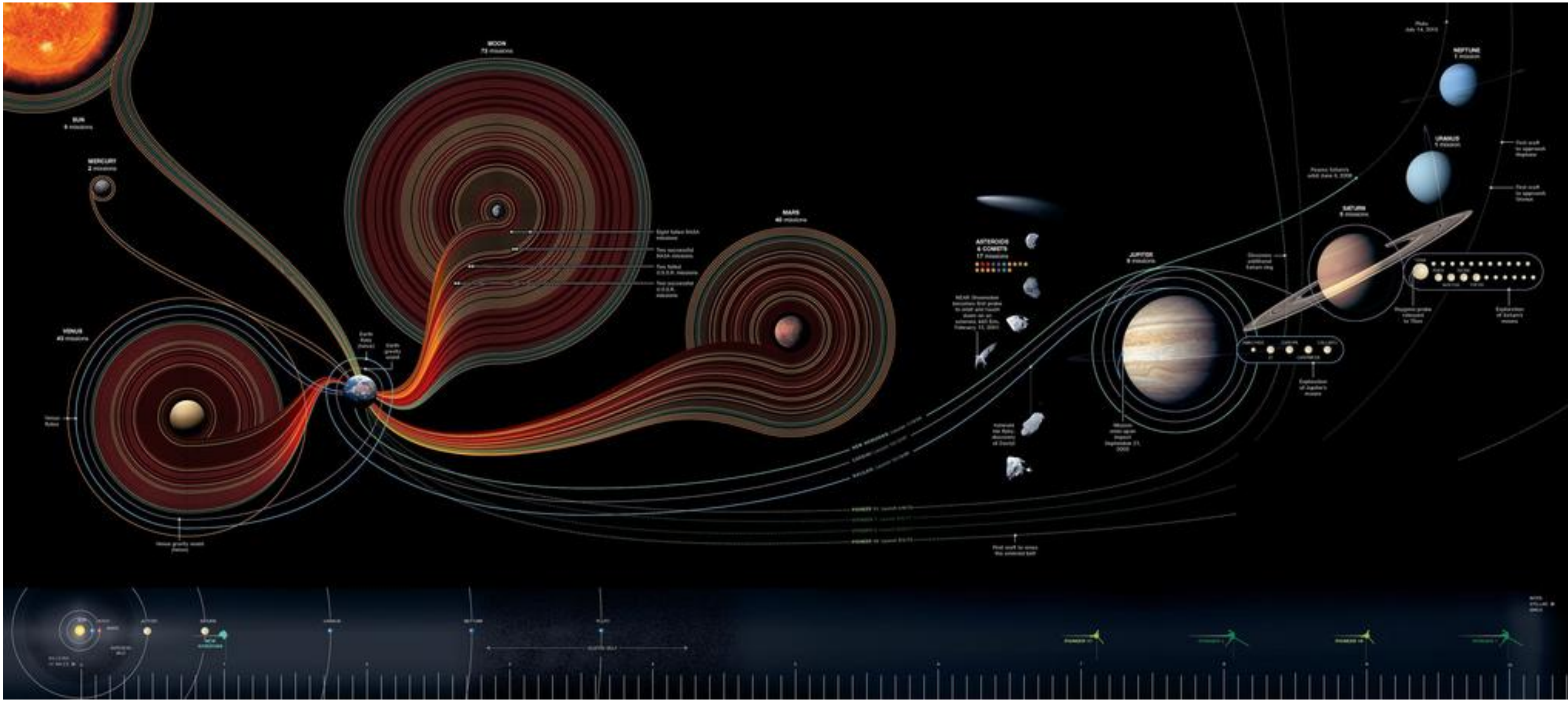

+ Moon: 73 missions

Mars: 40 missions

- Mercury: 2 missions (1974 & 2011)

Pluto: 1 misssion (in 2015)

Opportunity for image analysis

- Detections and/or delineations of geological structures and respective mapping have been based mainly on manual efforts, calling for sampling and subjective procedures

- Presently, images with much better resolutions (spatial, temporal and sometimes spectral) are available

- Serious attempts for developing automated methods are very recent (half-decade)

- It still is an open field for image analysis methods, in general

- Diversified nature of geological structures are ideal for Mathematical Morphology (MM)

Framework

- Remote study of teluric planetary surfaces of the Solar System

  - To analyse more recent data with better quality and in higher quantity

  - To reanalyse older data with more recent methods

- Characterization of structures and processes

  - Aeolian, glacial and periglacial, tectonic, vulcanic, impact,…

- Digital image analysis (with strong inputs from MM)

  - Development of automated robust methods, reproducible in different planetary surfaces in images obtained by different types of sensors (visible, infrared, radar,…)

- Use of terrestrial analogues as a reference for comparisons and extrapolations

Some examples of planetary structures under study

Impact craters
Mars, Moon, Mercury

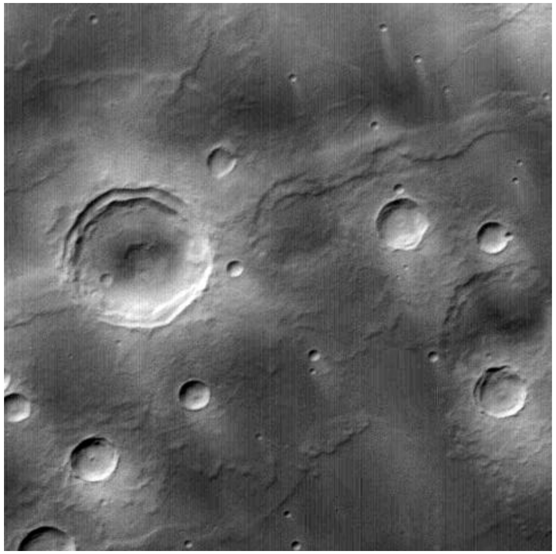

Polygonal terrains
Mars, Earth

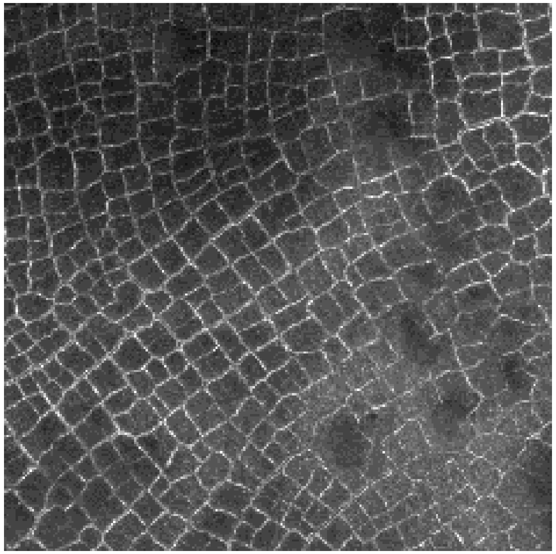

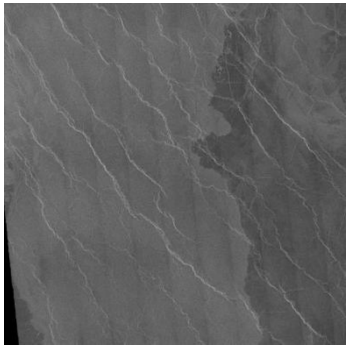

Wrinkle ridges
Venus

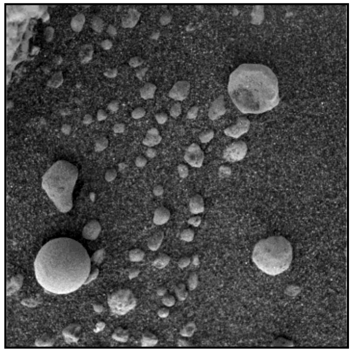

Soils
Mars

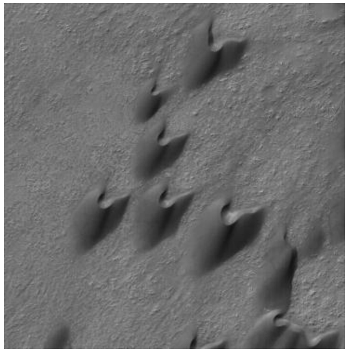

Dunes
Mars, Titan

Craters

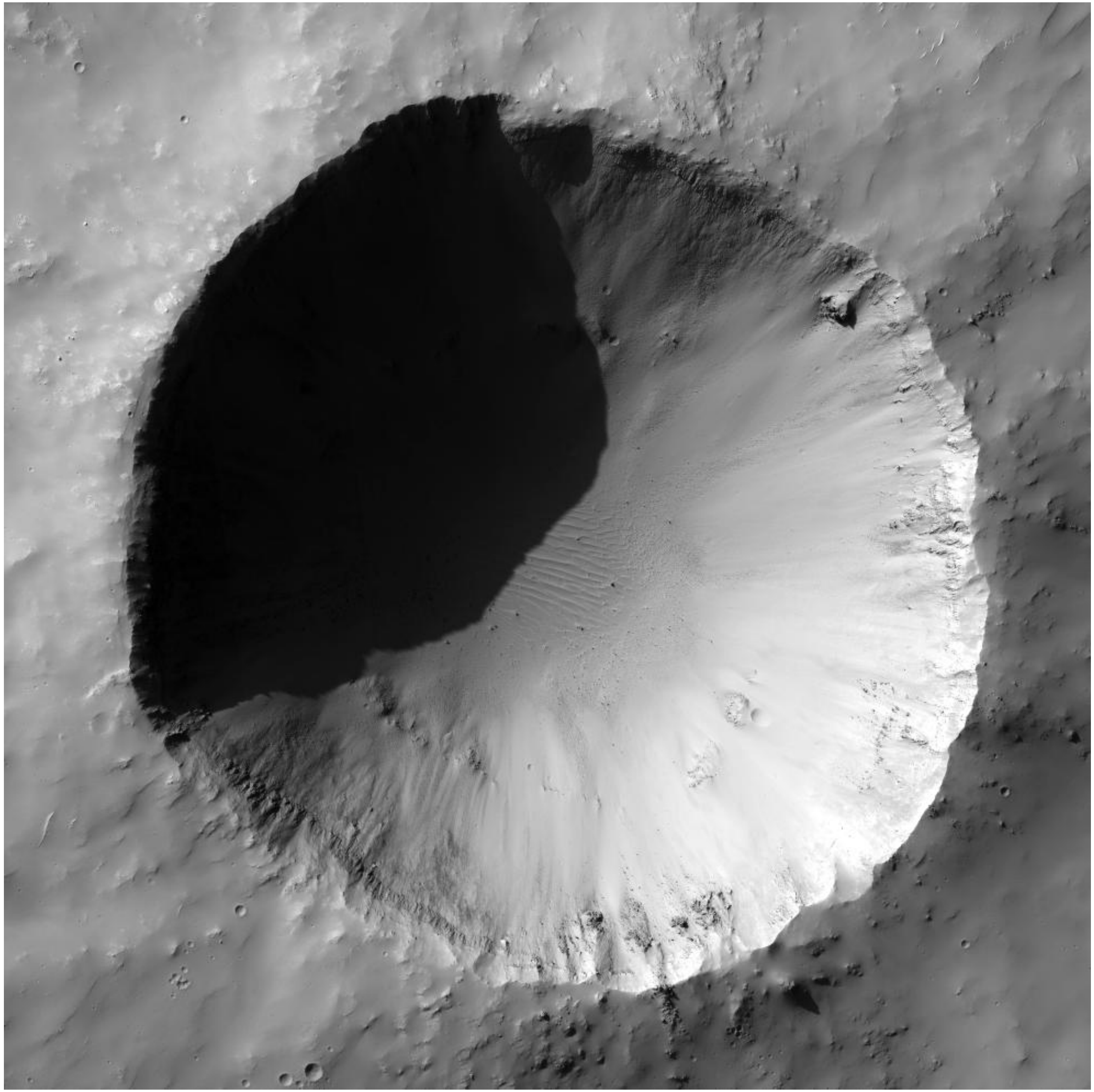

Geochronology by crater counting

Principle (Hartmann and Neukum, 2001):

The age of a terrain is directly proportional to the number of impact craters it contains, *i.e.*, a terrain with more craters is older than a terrain with less craters

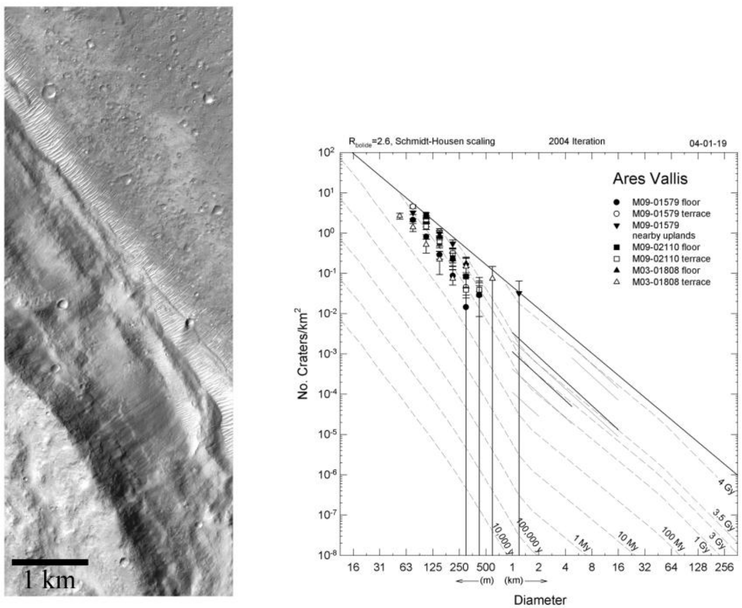

a b

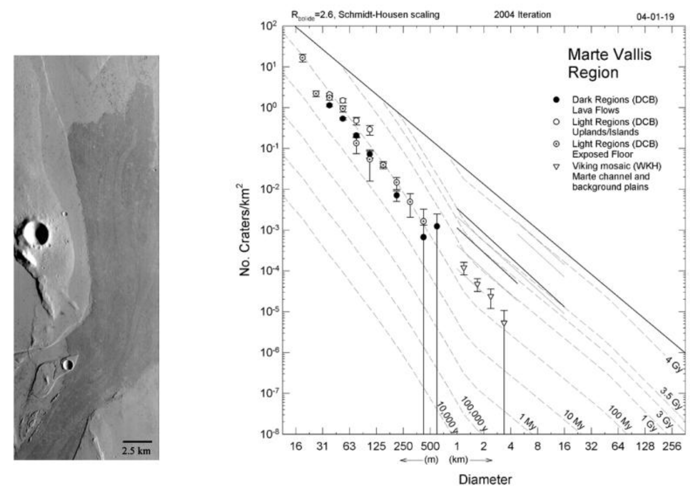

a b

Complete catalogue for Mars manually constructed (Barlow, 1988)

- about 40,000 craters > 5 km in diameter (D)

Digital image features

- Spatial resolution of images increased 10,000 times in 40 years: 3000 m/pixel (1965, Mariner 4) to 0.25 m/pixel (2005, MRO)

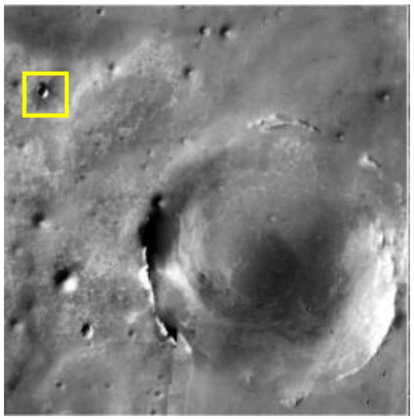

Victoria crater (Meridiani Planum)

THEMIS (18 m/pixel)

HiRISE (0.25 m/pixel)

Automated detection of impact craters

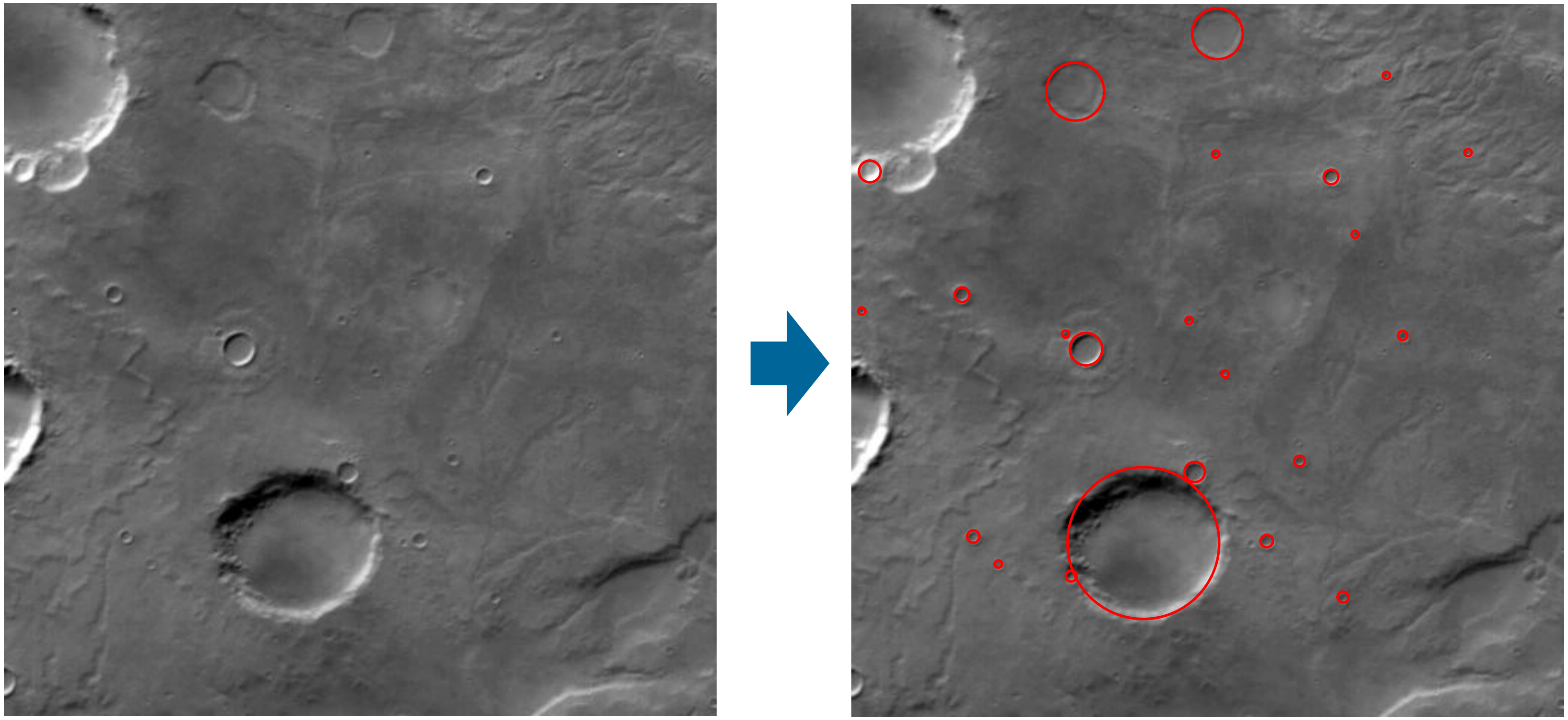

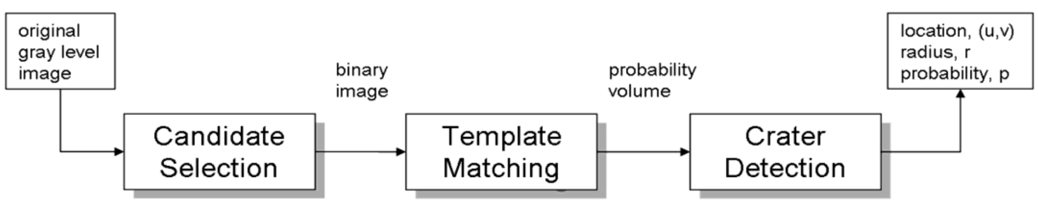

L. Bandeira, J. Saraiva, P. Pina (2007)
IEEE Transactions on Geoscience and Remote Sensing, 45(12): 4008-4015

Automated detection of impact craters

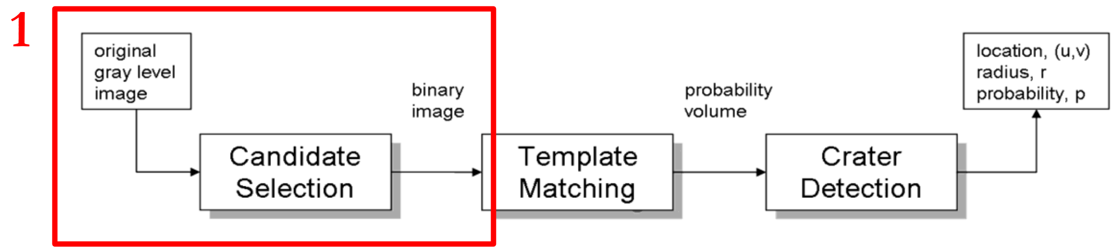

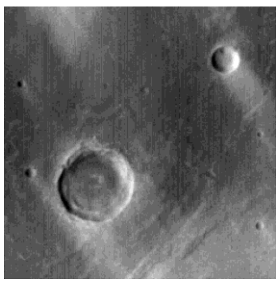

0. Input image:

MGS/MOC, 200 m/pixel, 8 bits

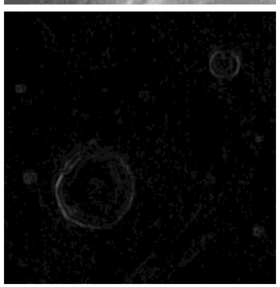

1a. Local enhancement (window 3x3):

$$A_{ij} = \max\left[m(M) - \min(M), \max(M) - m(M)\right]$$

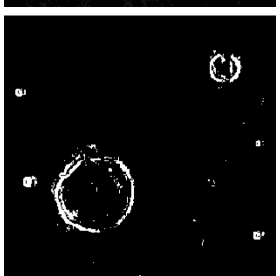

1b. Thresholding:

$$T = \alpha\left[\max(A) - \min(A)\right] + \min(A)$$

Automated detection of impact craters

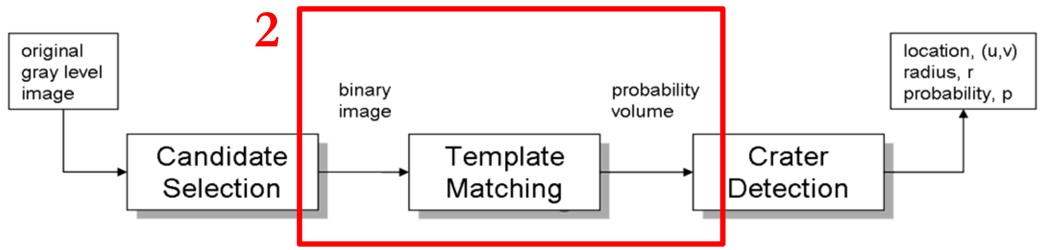

2a. Template matching with FFT-Fast Fourier Transform

2b. Construction of a probability volume

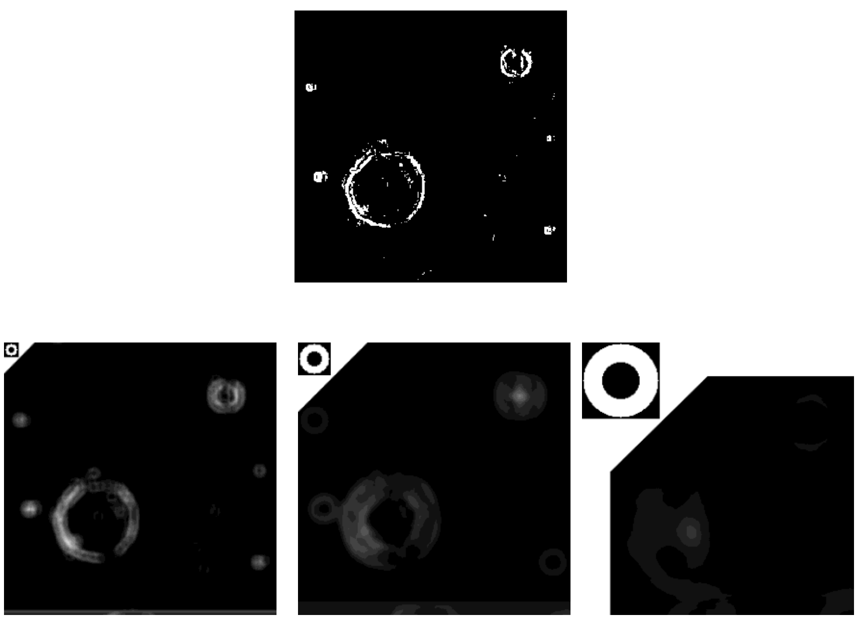

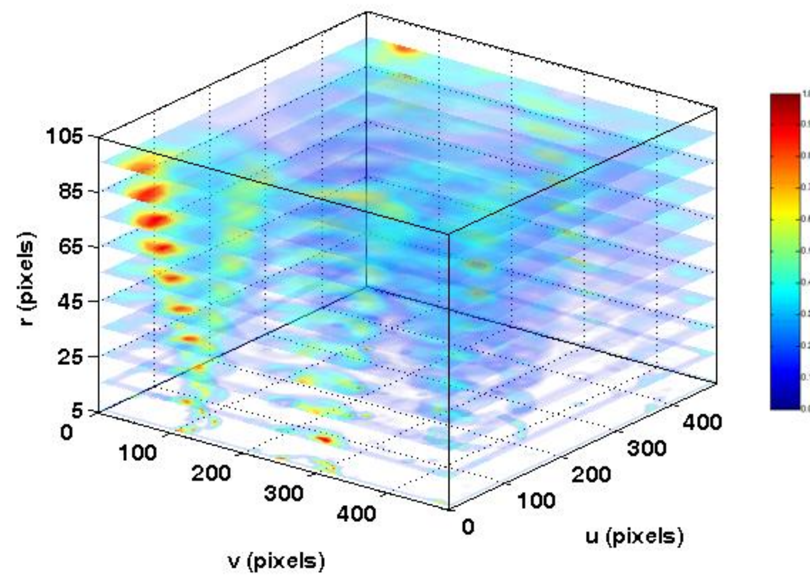

Automated detection of impact craters

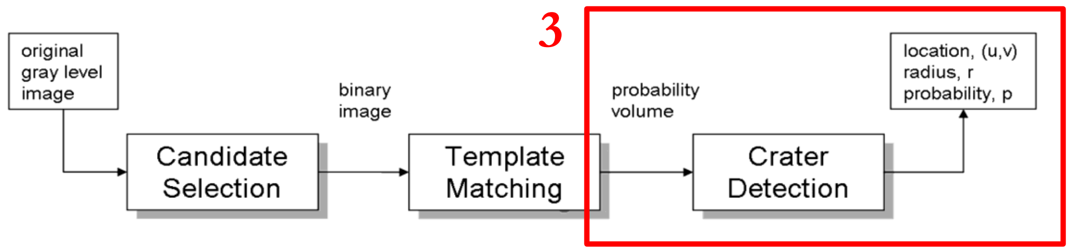

3a. Determination of regional maxima *M* on volume *P*:

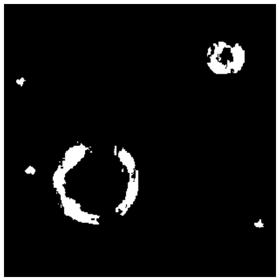

$$\begin{cases} \forall x \in M, P(x) = p \\ \forall y \in \delta^{(1)}(M) \setminus M, P(y) > p \end{cases}$$

$$RMAX(P) = P - R_P(P-1)$$

3b. Computation of extended maxima (EMAX):

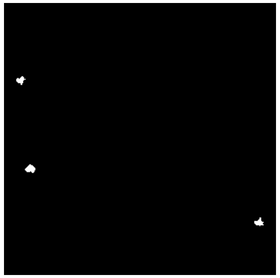

$$HMAX_h(P) = R_P(P-h)$$

$$EMAX_h(P) = RMAX_f(HMAX_h(P))$$

3c. Filtering:

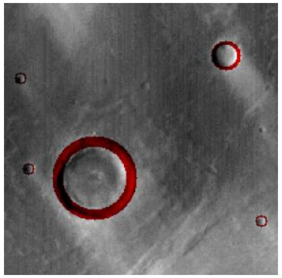

Area-opening $\gamma_\lambda(W) = \left\{ w \in W : Area\left[C_w(W)\right] \geq \lambda \right\}$

Circularity $CI = 4\pi.Area / Perimeter^2$

Detection examples (D > 2000 m)

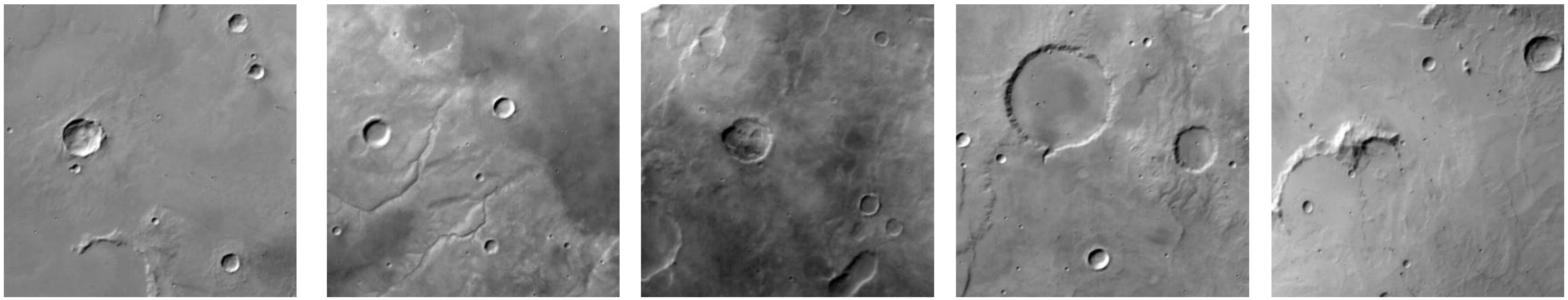

MOC R01-01374 | MOC R02-00575 | MOC R02-00830 | MOC R02-00837 | MOC R02-00872

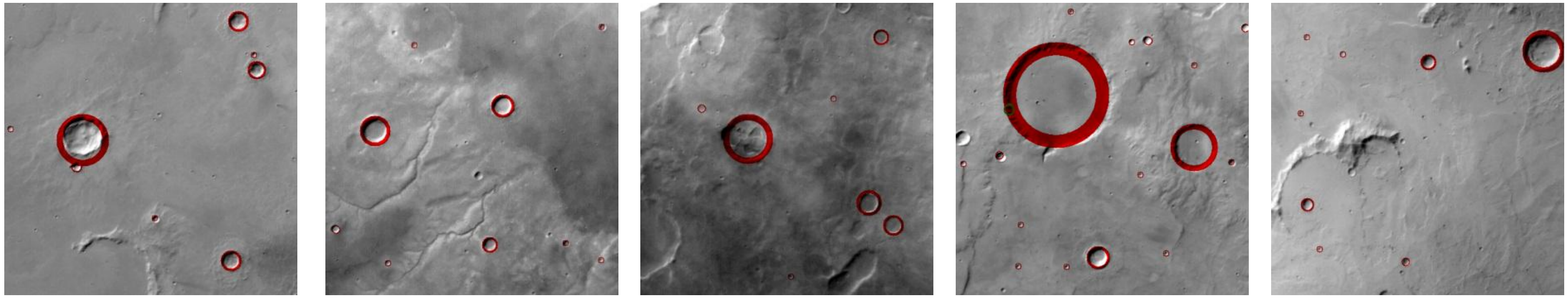

88% | 79% | 88% | 89% | 83%

Images: NASA/JPL/MSSS

Large scale validation – Same stratigraphic unit

Testing with a large set of images with well-known (crater density) characteristics

Reg	(1)	(2)	(3)	(4)	(5)
A	290ºE-40ºN	295ºE-35ºN	27	13	11
B	290ºE-20ºN	300ºE-10ºN	74	37	18
C	280ºE-15ºS	290ºE-25ºS	37	17	9
D	110ºE-20ºS	120ºE-30ºS	159	88	63
Total			297	155	**101**

Hr unit – Ridged plains (Scott & Carr 1978)

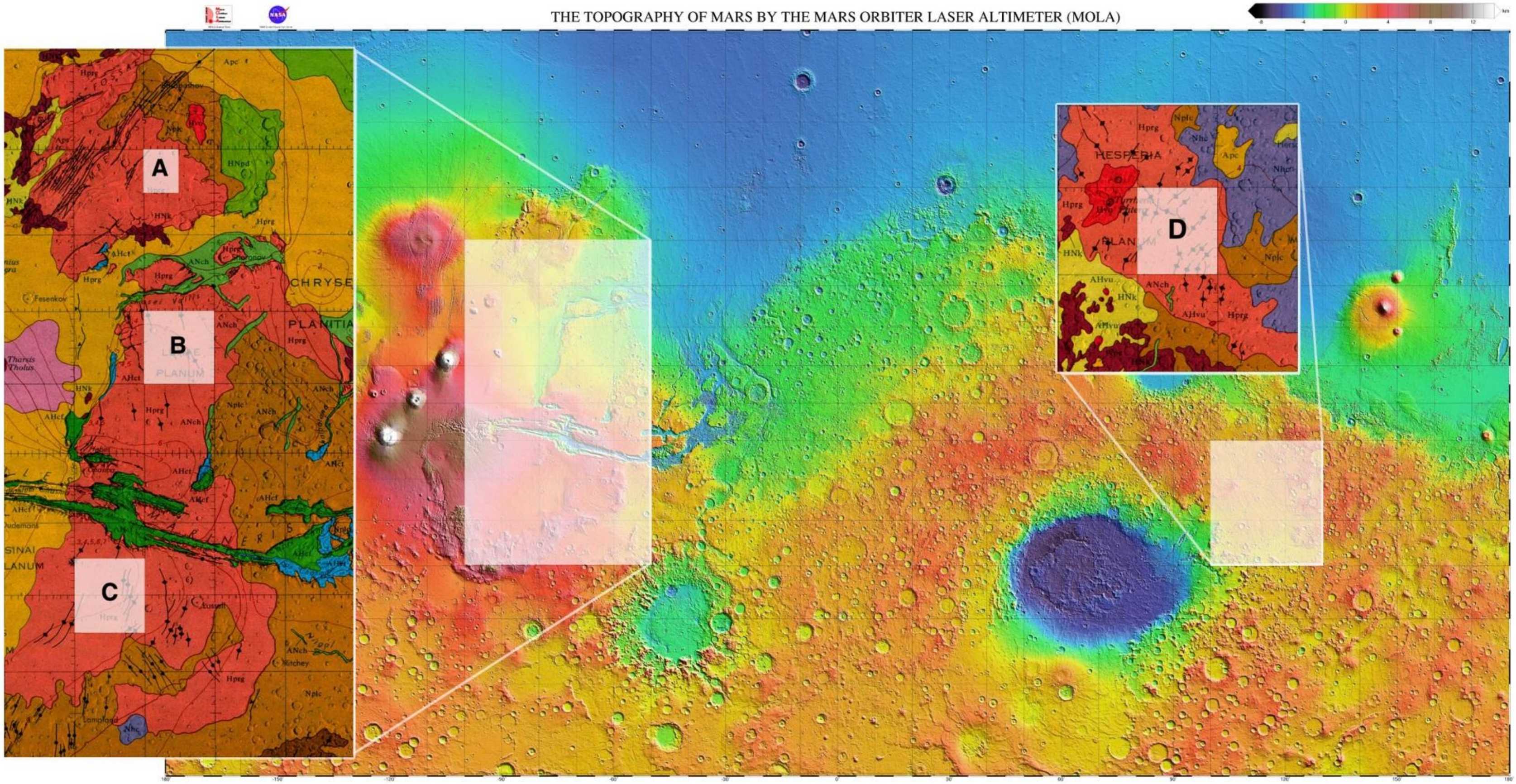

Large scale validation – Same stratigraphic unit

E19-00650

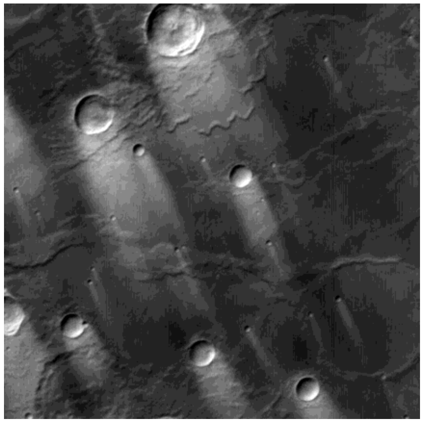

p=0.30

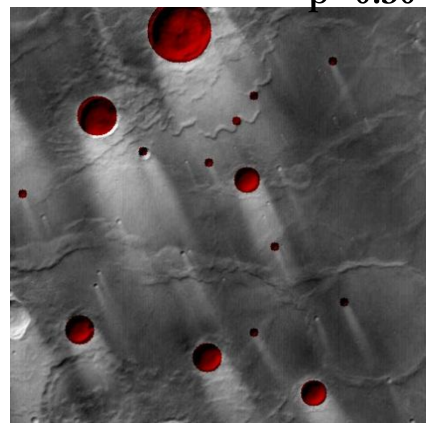

p=0.45

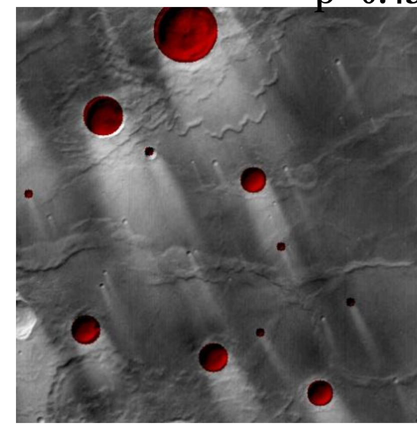

Dependency of the results on the level of probability **p** selected

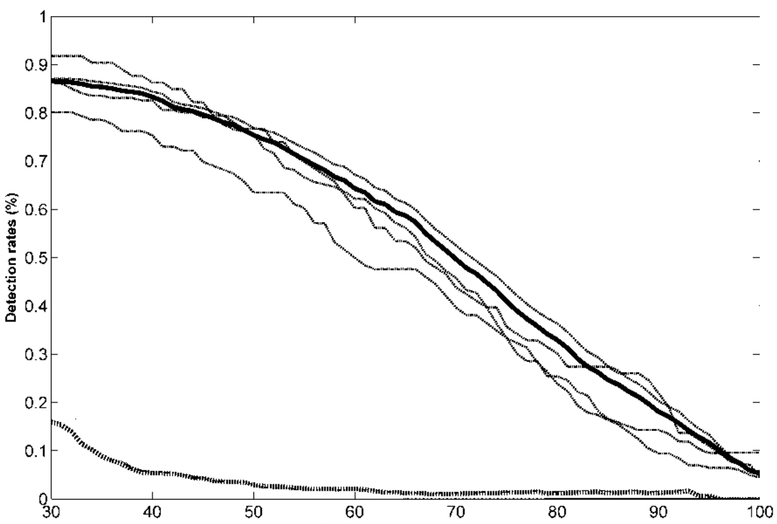

Region	*GT* (#)	TD_{30} (#)	TDR_{30} (%)	FD_{30} (#)	FDR_{30} (%)
A	126	101	80.16	24	19.20
B	201	174	85.57	17	22.99
C	73	67	91.78	20	8.90
D	872	759	87.04	148	16.32
Total	**1272**	**1101**	**86.57**	**209**	**15.95**

Crater density: 174 per 10^6 km^2

(130-200 in bibliography)

Large scale validation – Different stratigraphic units

Region around Gusev crater, Southern hemisphere, near the equator

Image H2729_0000_ND3 (HRSC/DLR/GNeukum/FUB

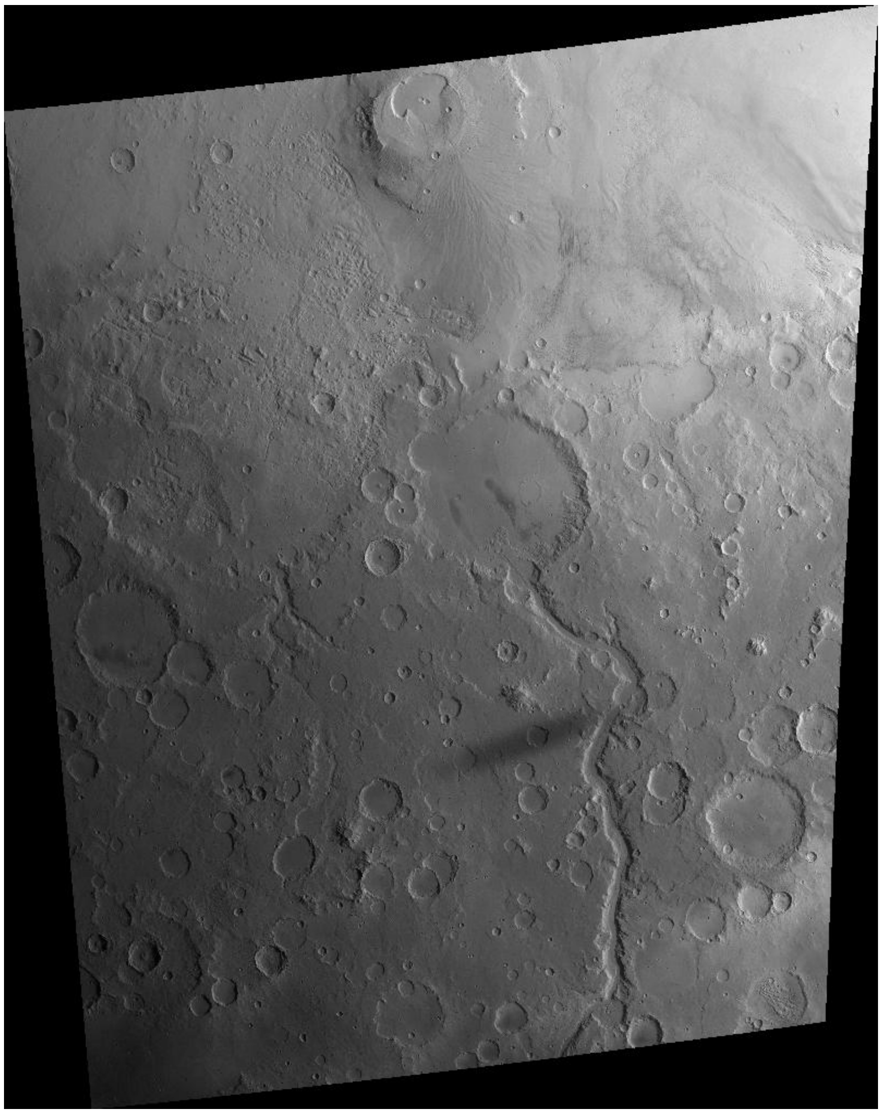

Close to the dichotomy border and covering formations of diverse age

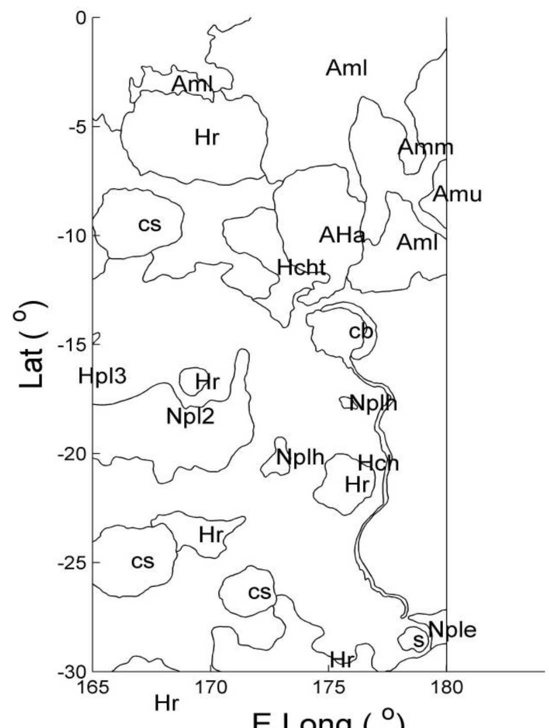

Large scale validation – Different stratigraphic units

Survey of images available

red - MGS/MOC

blue - Odyssey/THEMIS

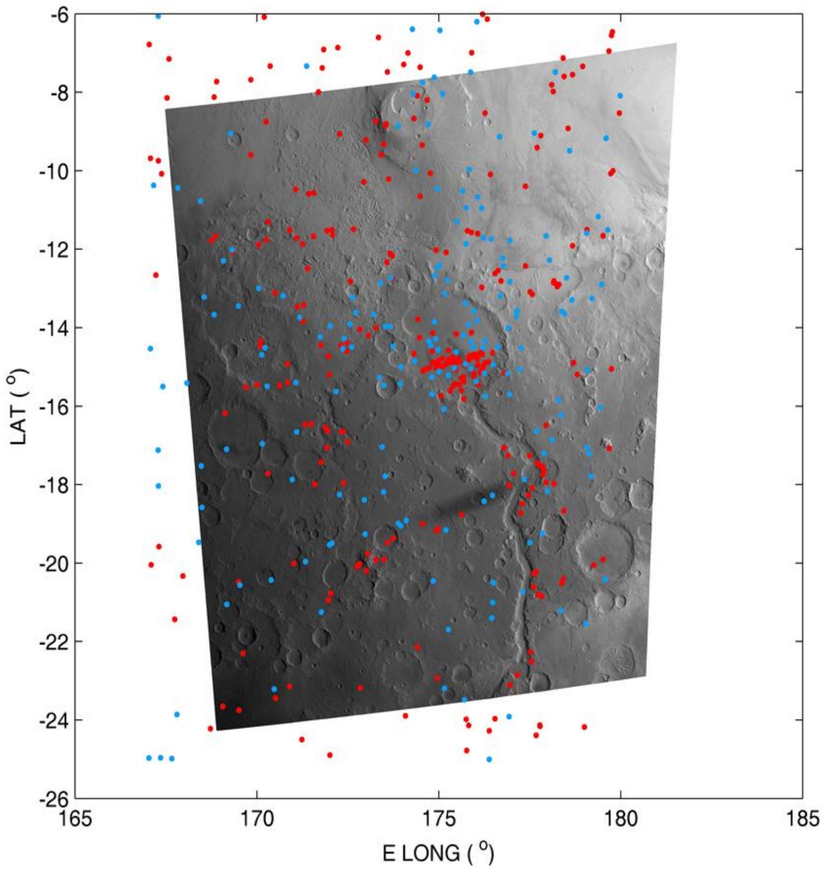

Image footprints

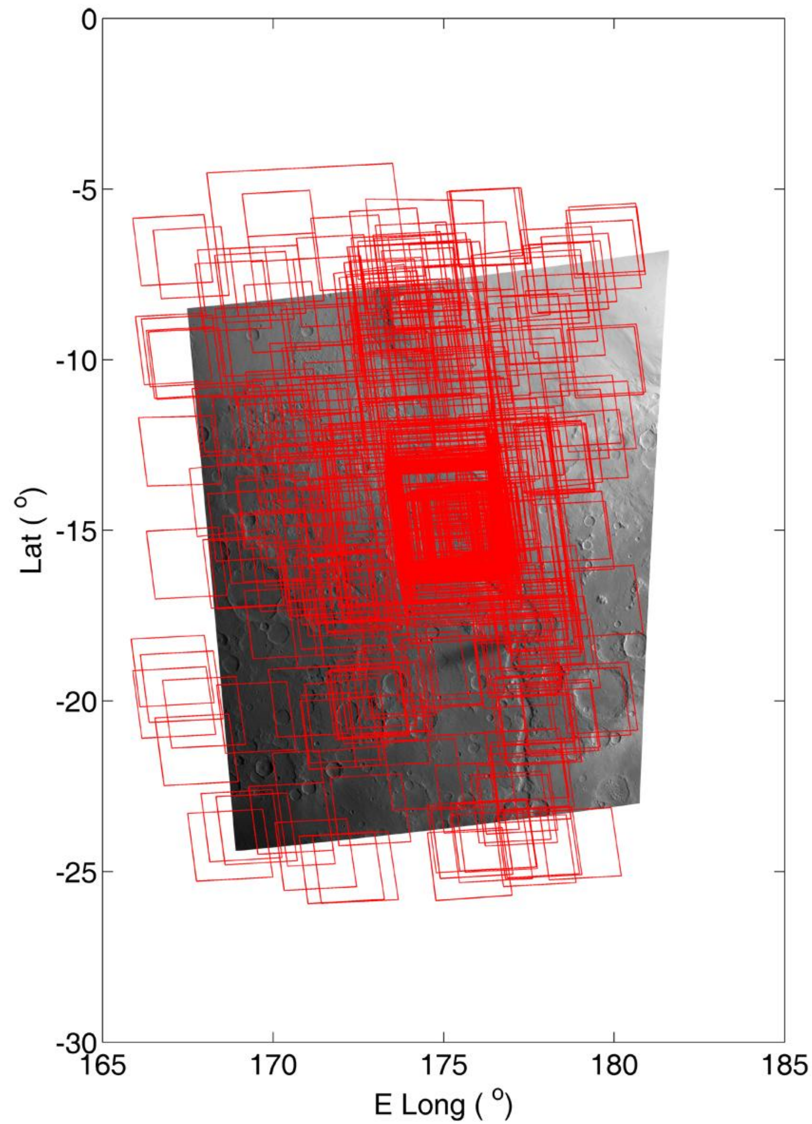

Large scale validation – Different stratigraphic units

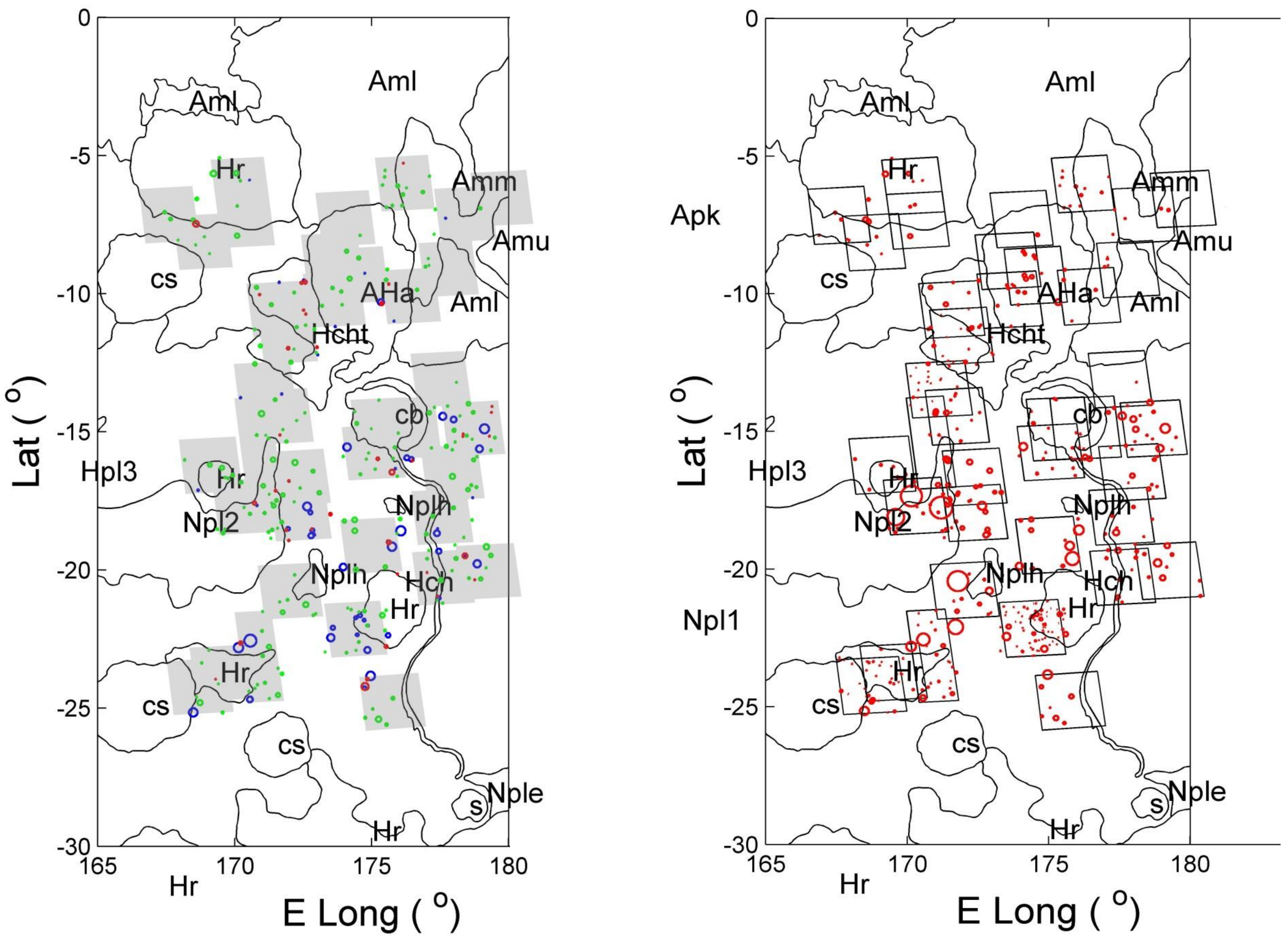

Large scale validation – Different stratigraphic units

- Older formations are more cratered and images are more cluttered: they present lower performances

Formation	Age	TDR	FDR
Am	Amazonian	0.74	0.08
Apk	Amazonian	0.86	0.08
AHa	Hesperian	0.93	0.35
Hcht	Hesperian	0.71	0.33
Hr	Hesperian	0.84	0.25
Npl1	Noachian	0.65	0.35
Average		*0.73*	*0.28*

Mostly **Noachian**

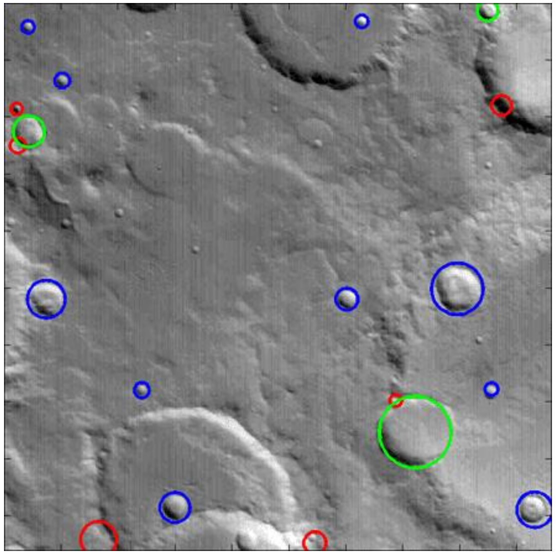

M17-01195

Mostly **Hesperian**

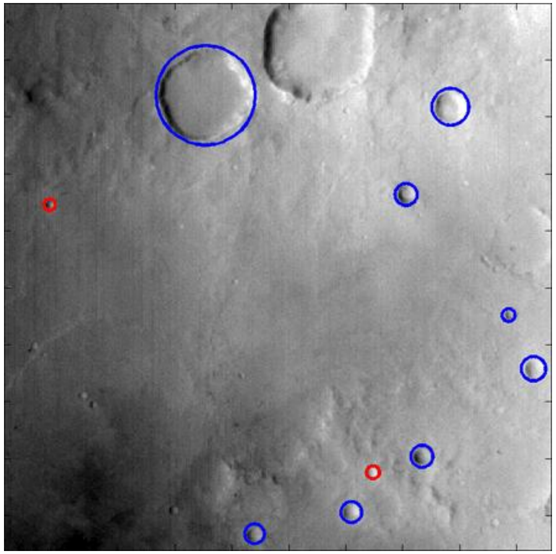

R12-02650

Mostly **Amazonian**

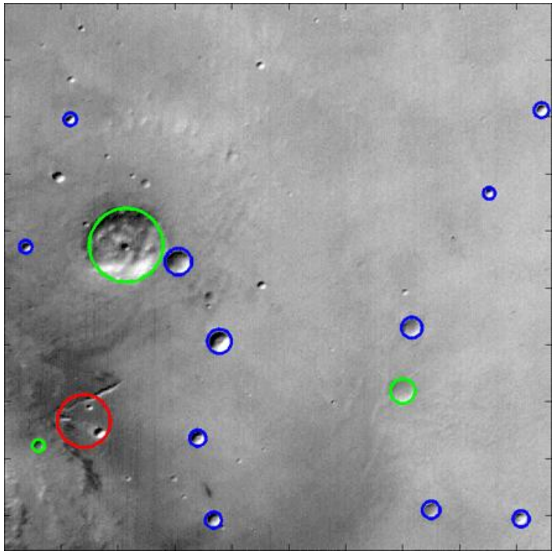

E23-01177

Images: NASA/JPL/MSSS

Catalogue

- Convergence towards an unified catalogue of Martian craters

- Completation of existing catalogues mainly based on DTM-Digital Terrain Models (MOLA) with outputs from CDA-Crater Detection Algorithms on optical images

- Craters D > 2000 m

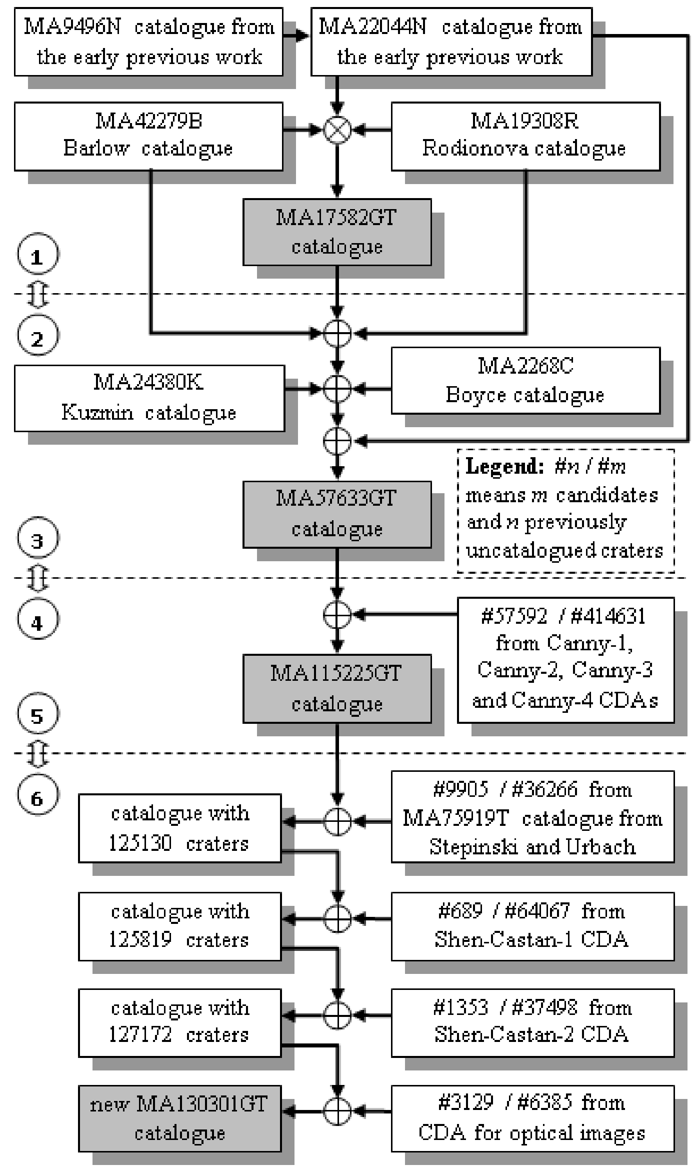

Detection of metric craters (D > 2.5 m)

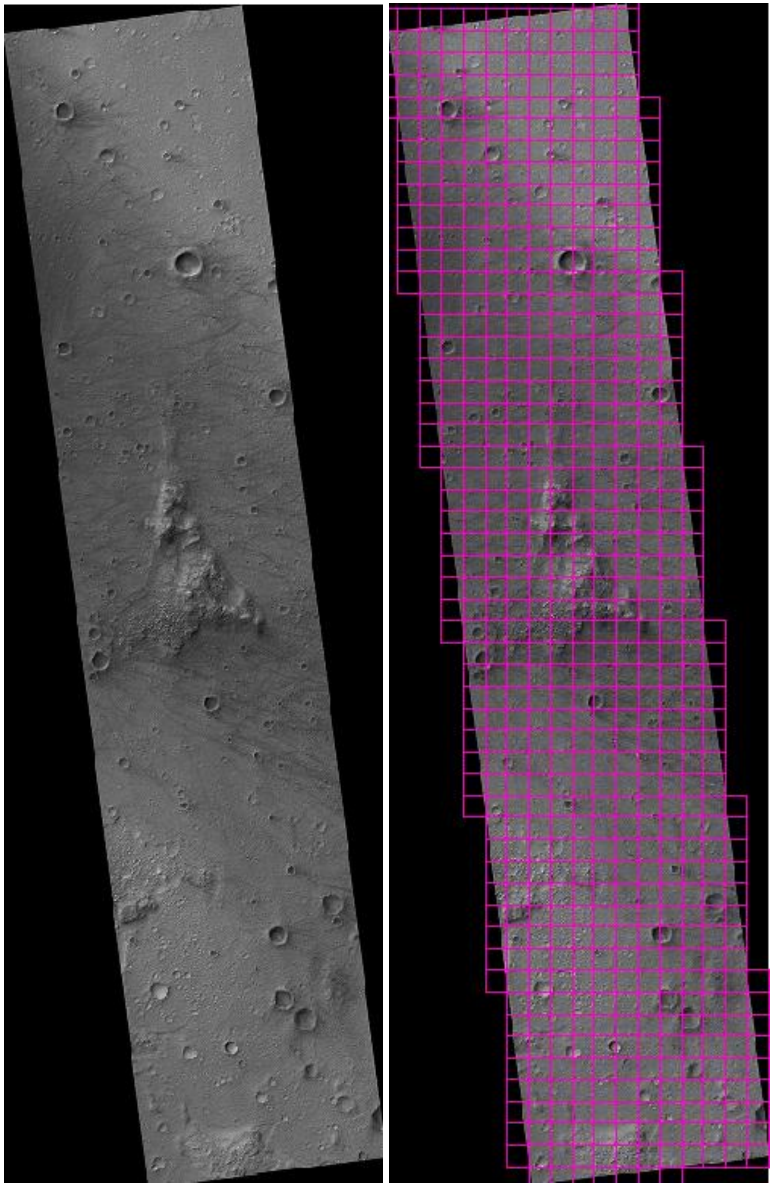

MRO/HiRISE - 108,029 x 34,839 pixels ≈ 27.07 x 8.71 km^2

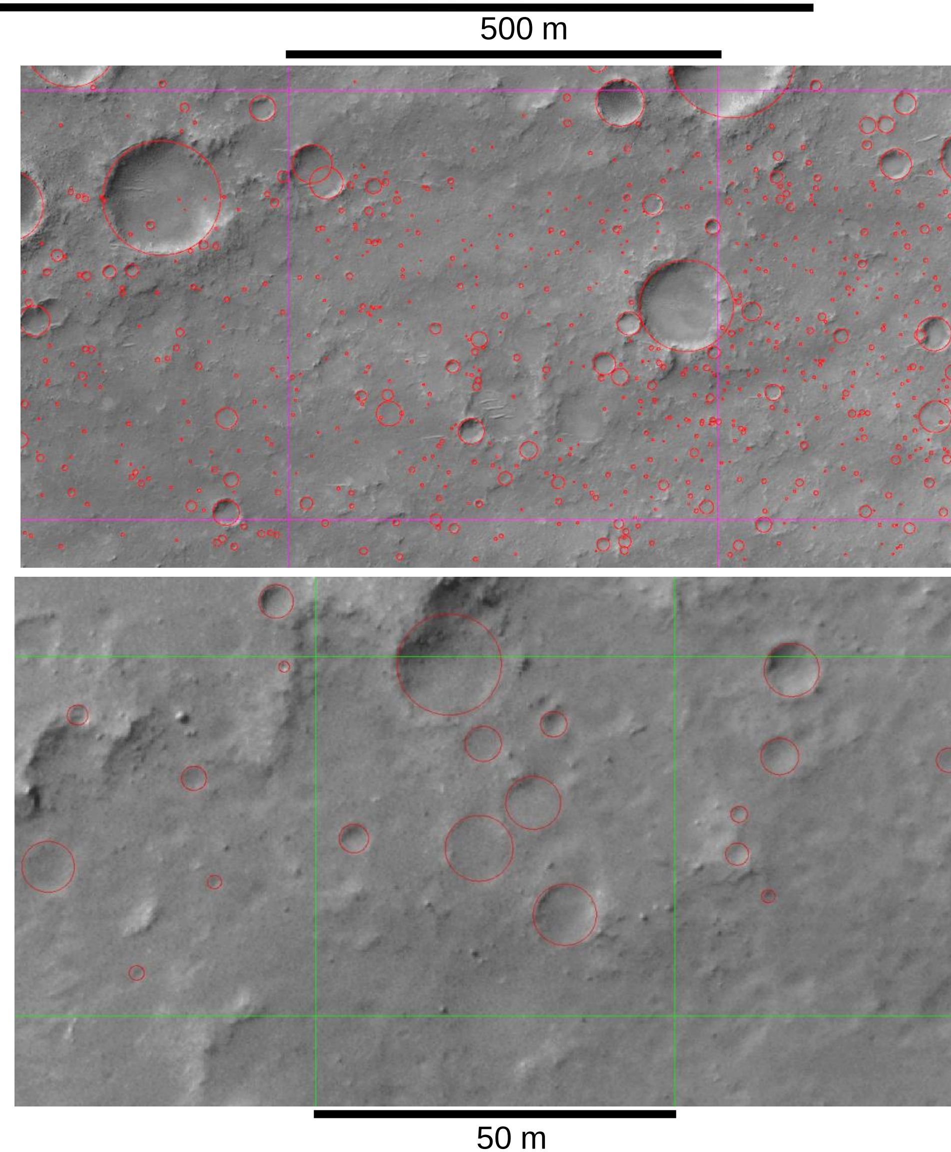

PSP_009174_1650: more than 170,000 craters

Polygons

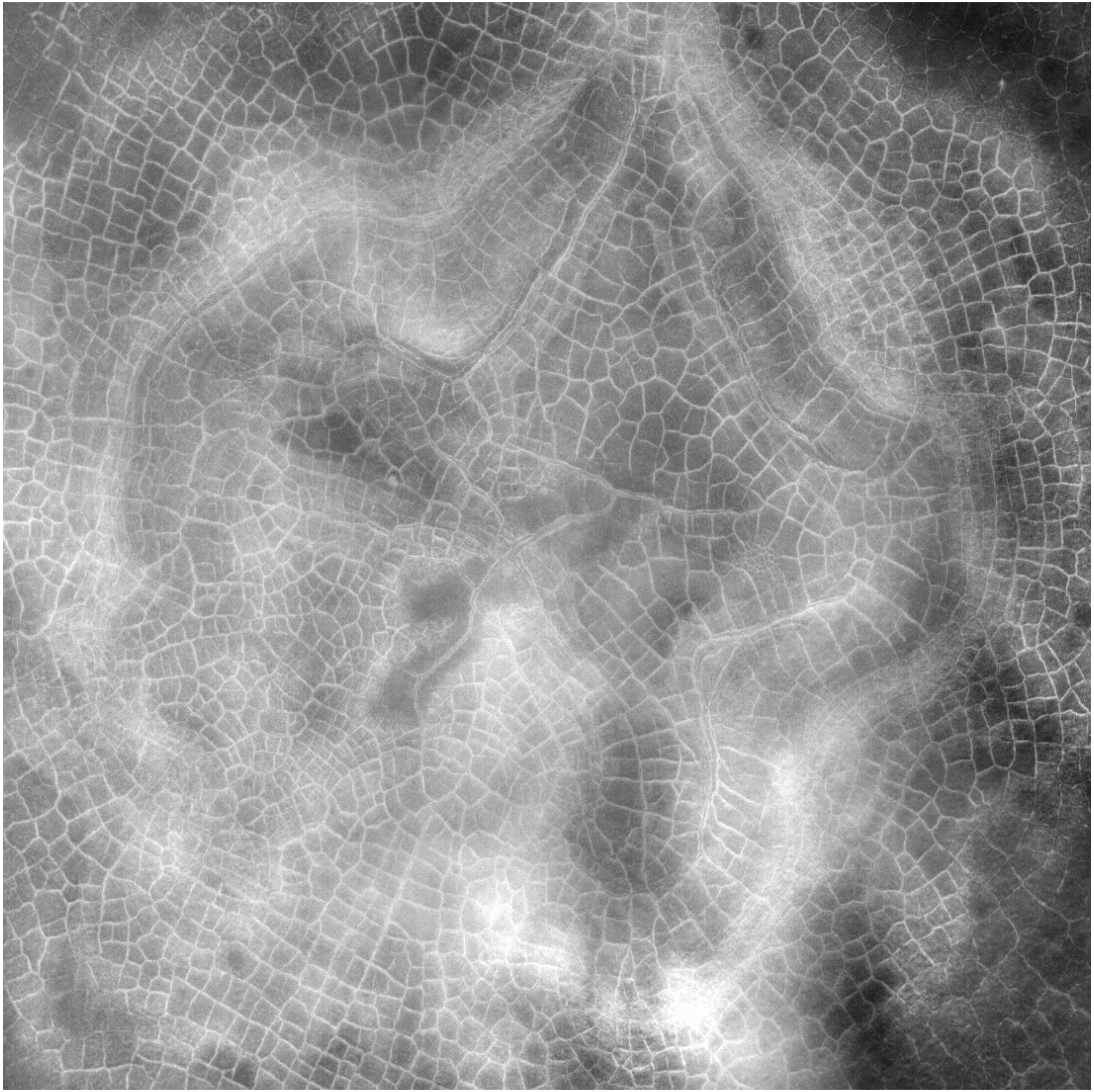

Studies of polygonal patterns on Mars

Discovery
- 1970s: Large scale (km) – Tectonics
- 2000s: Small scale (30-400m) – Periglacial origin with seasonal thermal contraction of terrains

Location
- Survey of images (Seibert & Kargel 2001, Kuzmin & Zabalueva 2003)
- Relate with ground ice (Mangold et al. 2004; Kuzmin et al. 2004)

Characterization
- Measure parameters (geometric, few topological) (Yoshikawa 2003)

Classification
- Constitute clusters based on few similarities (Mangold 2005, Levy 2008)

Methodologies employed?
- Visual inspection, manual contouring
- Network sampling with limited number of polygons evaluated!

Gathering data: Image survey on Mars

- Mars Global Survey / Mars Orbiter Camera [na] images
- 1998 to 2006, above 50º (N and S), 1.5 – 6.0 m/pixel
- **15855 images evaluated, 1184** containing **polygonal networks**

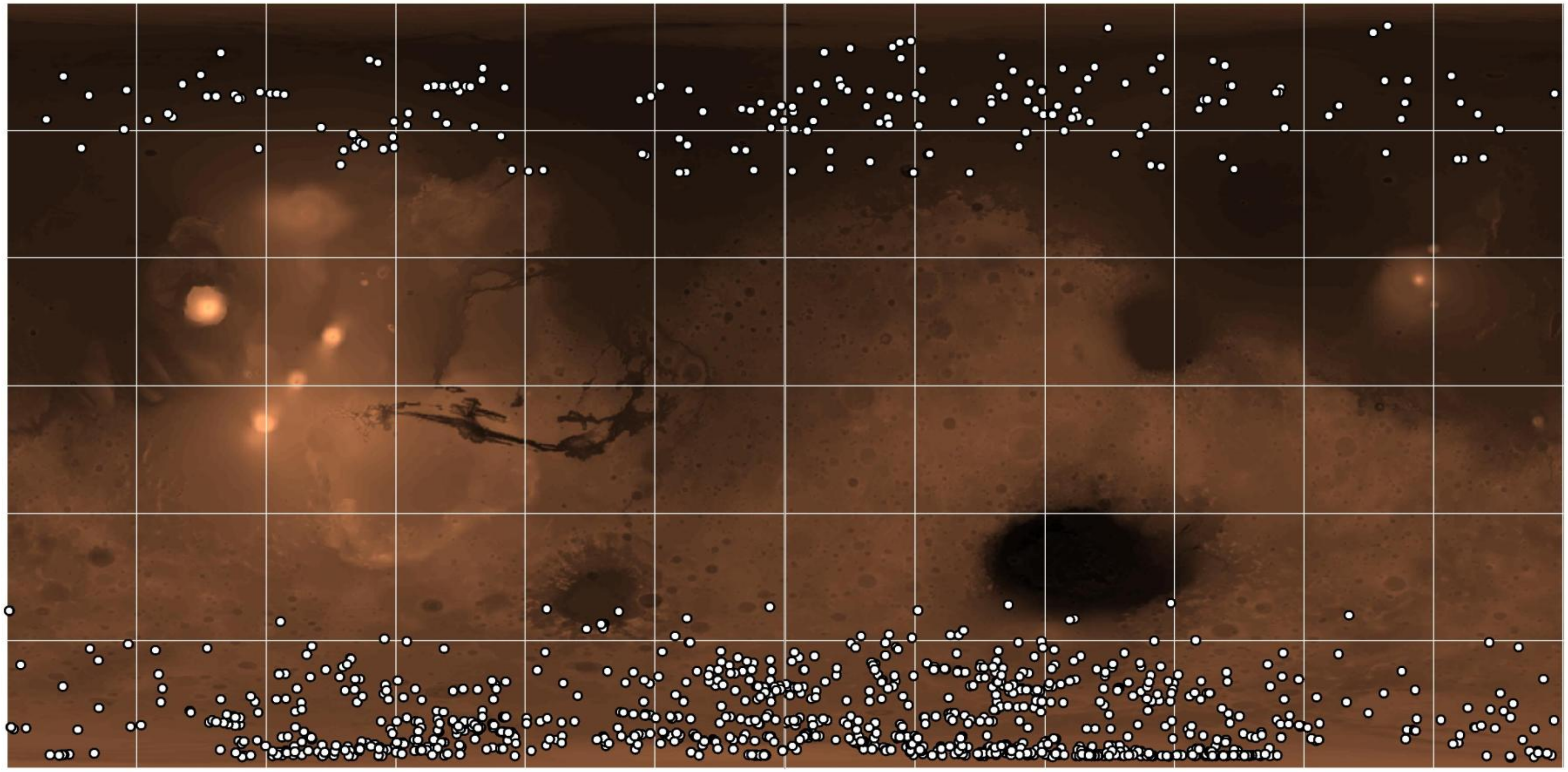

Selection of networks for analysis

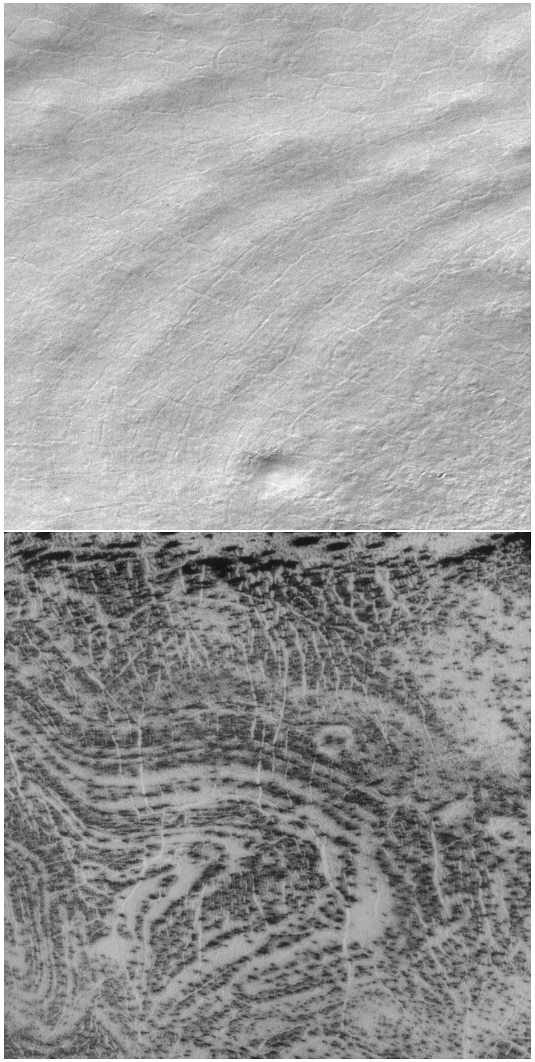

There are many examples of polygonal networks that are not suitable for the direct application of an automated methodology

Only **clearly discernible and extensive networks** were used.

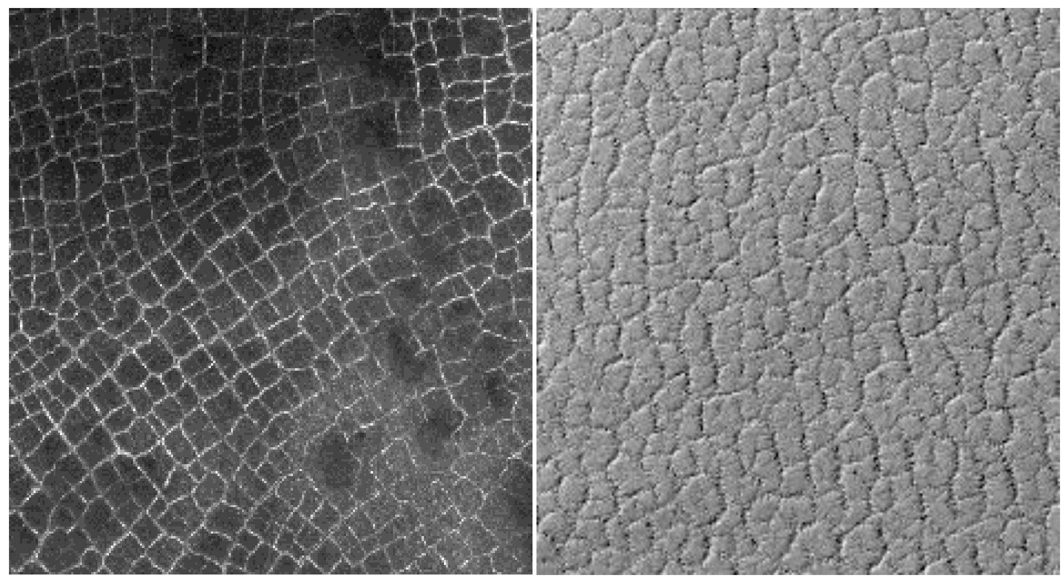

Mosaic of Martian polygonal networks

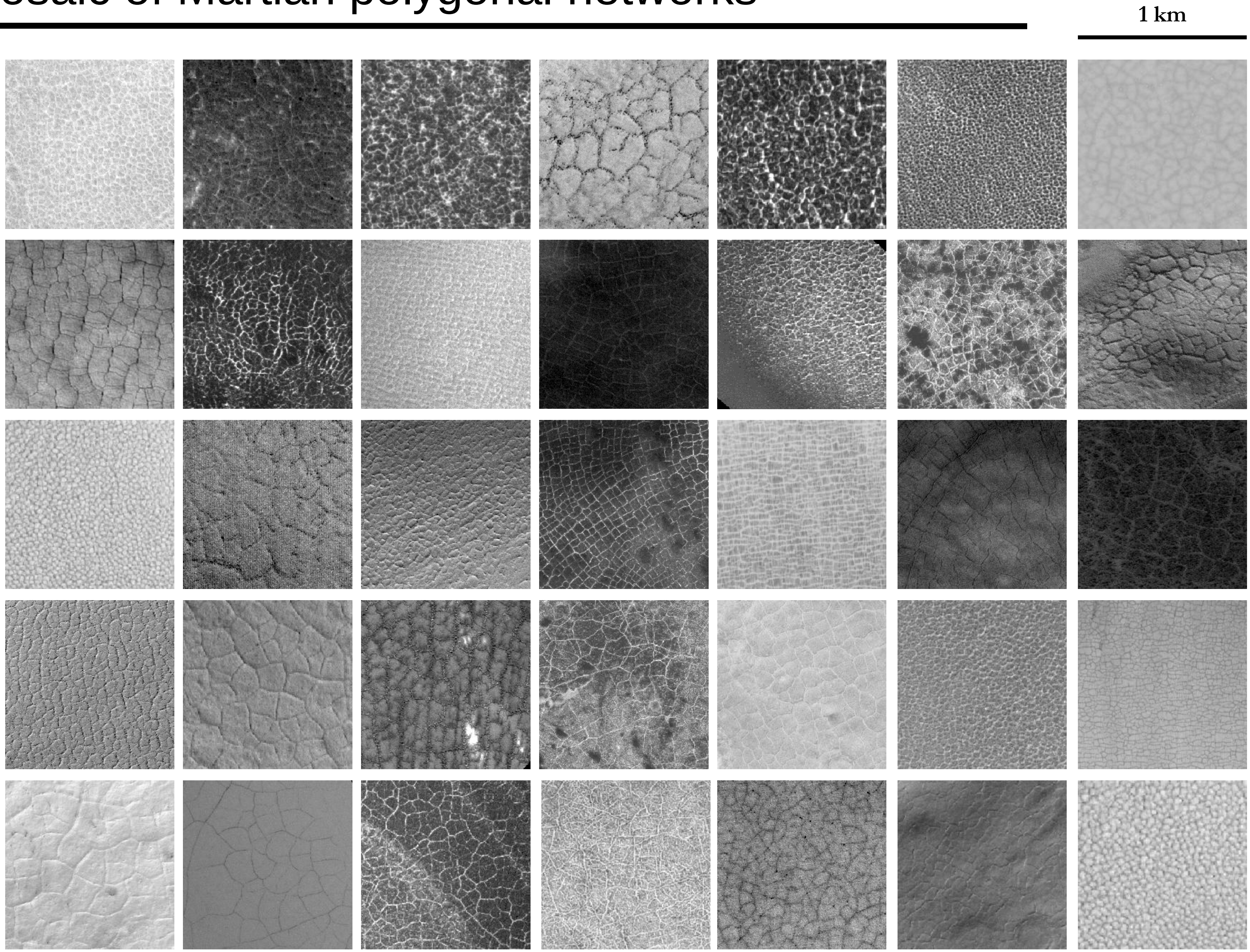

Automated approach

- To construct a single approach that is able to identity, characterize and classify all types of patterned terrains

1 Image Segmentation

1. Morphological filtering;
2. Segmentation: by watershed
3. Contour Selection by dynamics

2 Feature Extraction

Geometric/dimensional features: area, shape, orientation…

Topological features: neighbourhood analysis

3 Clustering and Classification

To analyse an *n*-dimensional feature space with Multivariate Data Analysis and Pattern Recognition approaches to detect clusters of polygonal terrains that can lead to an objective classification into distinct patterns.

Image segmentation

1. Filtering: Morphological filtering by reconstruction (Opening/Closing)

$$\varphi_R^{\lambda}(f) = R_f^{\varepsilon}\left[\delta^{\lambda}(f)\right] \qquad \gamma_R^{\lambda}(f) = R_f^{\partial}\left[\varepsilon^{\lambda}(f)\right]$$

2. Segmentation: Watershed transform (Beucher and Lantuéjoul 1979)

$$WS(f) = SKIZ_f\left[\min(f)\right]$$

3. Contour Selection: Analysis of watershed contours through their dynamics (Najman and Schmitt 1996)

$$dyn(C) = \min[I(s) - m_i]$$

Image segmentation

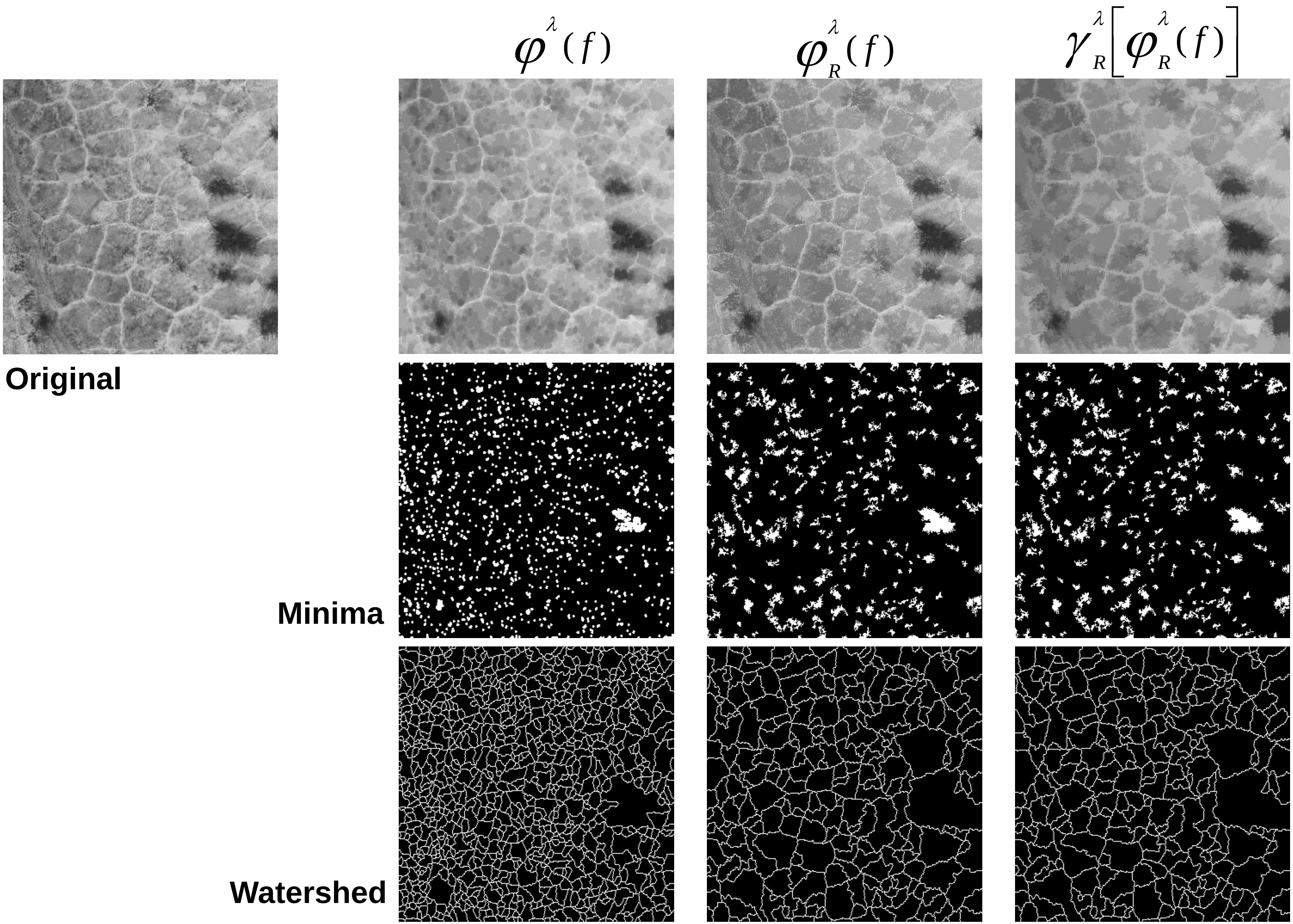

Image segmentation sequence

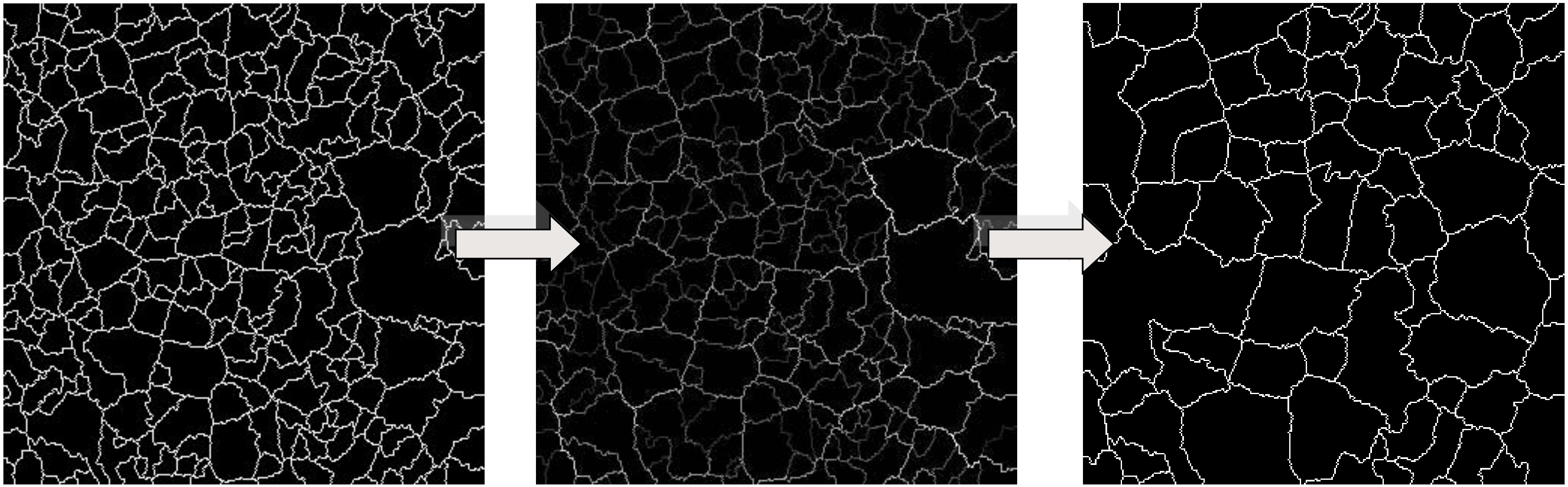

Watershed

Contours dynamics

Selected contours

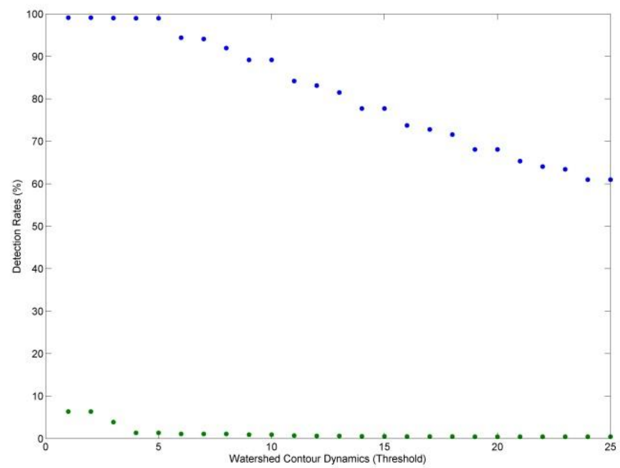

Segmentation performance

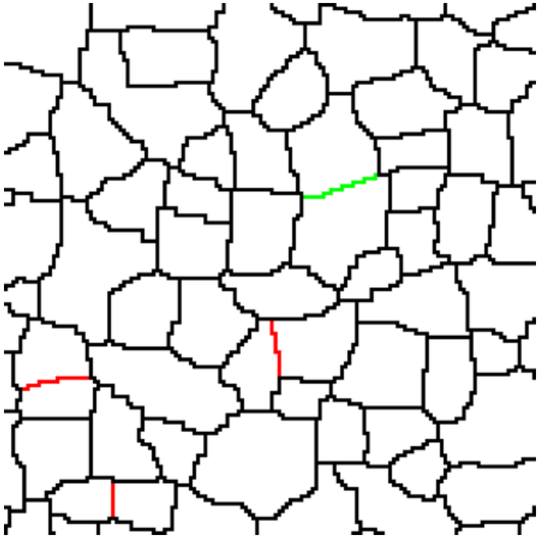

- Comparison between automated result and interpretation of original image (ground-truth)
- Pixels are classified as
  - **tp**: part of a polygon's contour (black)
  - **tn**: part of a polygon's interior (white)
  - **fp**: wrongly part of a polygon's contour (red)
  - **fn**: missed contour (green)

- Overall performance $Gmean = \sqrt{\dfrac{tp \cdot tn}{(tp + fp) \cdot (tn + fn)}}$

- The resulting value for 35 images varied for each one but with high performances (Gmean > 0.9):
  - **tp** always > 90%
  - **fp** always < 10%

Networks features

- **Geometric or dimensional**
  - Size and perimeter
  - Main and minor axis, shape factors, convexity
  - Orientation
  - Type of vertex: trivalent or tetravalent
- **Topological**
  - Number of neighbours of each polygon i
  - Number of neighbours of the neighbours of each polygon m_i

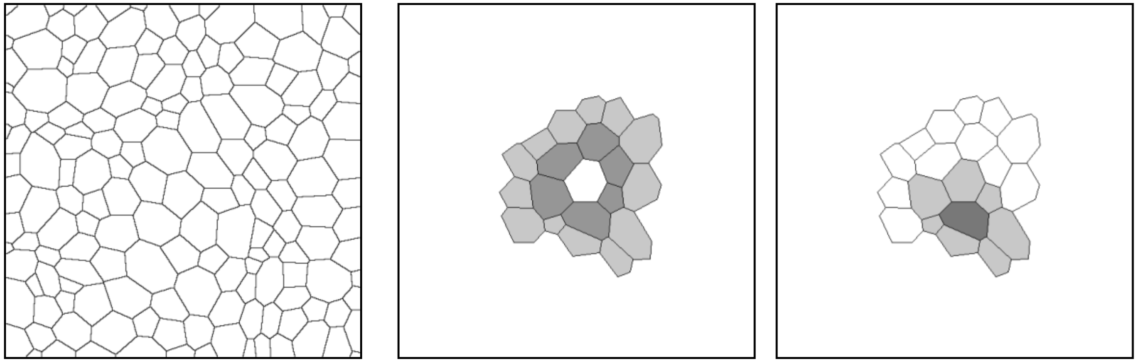

i m_i

Topological features I

Lewis law (1928, 1930)

• Pioneering studies on biological tissues (cucumber and amnion skins)

• Declares a linear connection between the average area $<A>_i$ of polygons with *i* neighbours in two dimensional tissues:

$$<A>_i = <A>[1+\lambda(i-6)]$$

i - Number of neighbours

$<A>_i$ - Average area of polygons with *i*-neighbours

$<A>$ - Average area

λ - Network constant

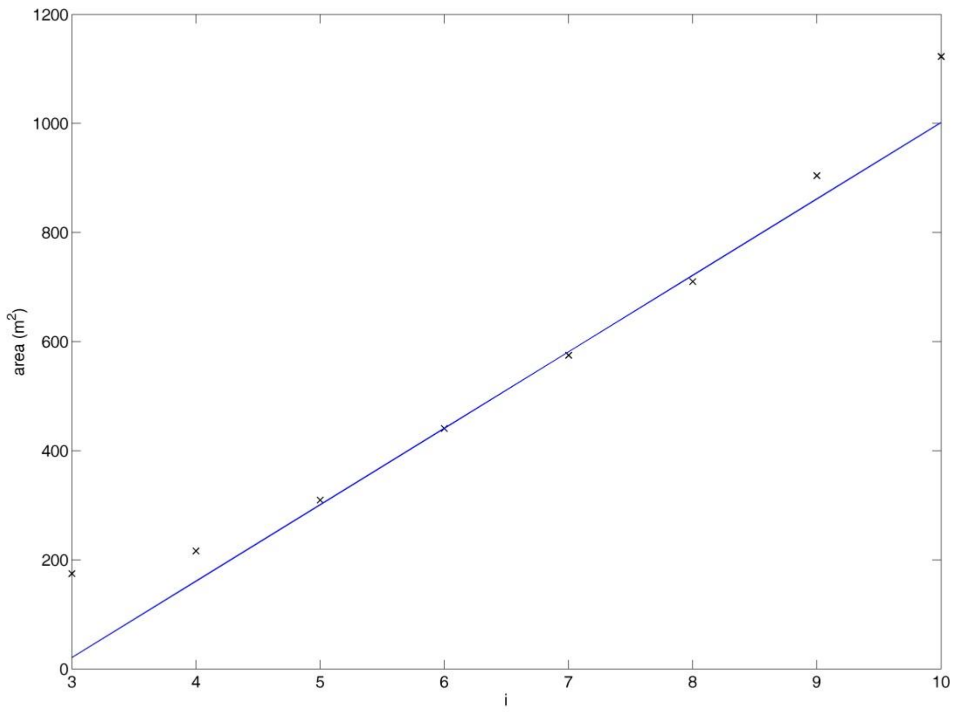

Topological features II

Aboav-Weaire law (1970, 1984)

• The recognition of fundamental similarities between biological tissues and other cellular systems (soap froths and polycrystals) permitted to establish other type of correlations

• The average number of sides in polygons adjacent to *i*-polygons is linear:

$$m_i = 6 - a + \frac{6a + \mu_2}{i}$$

i - Number of neighbours

m_i - Average poligonality of *i*-neighbours

μ_2 - 2nd moment

a - Network constant

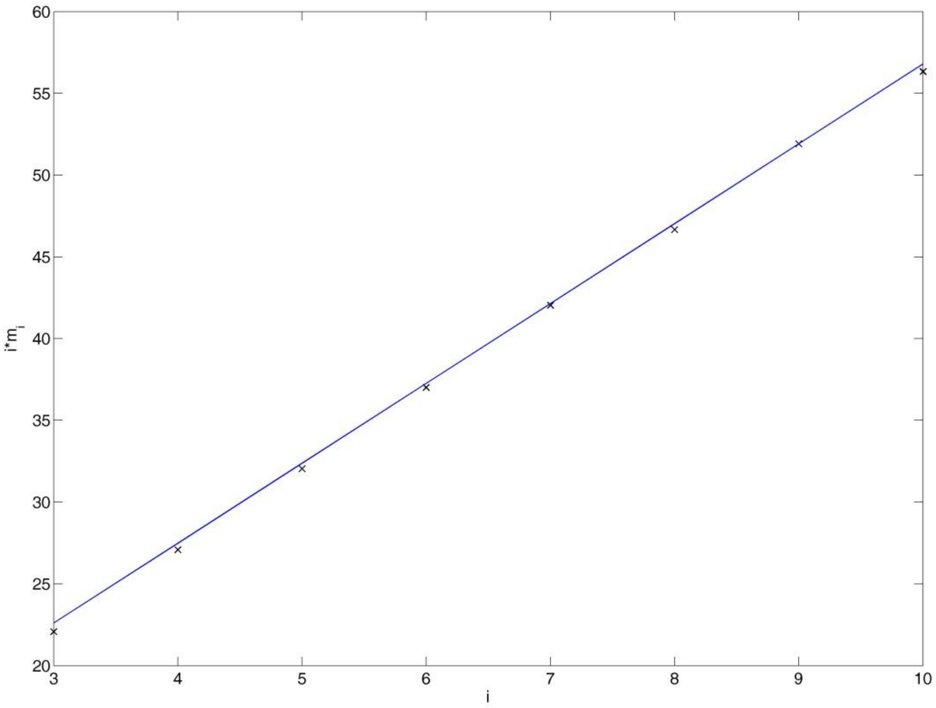

Computing topological features on huge networks

- Northern plains of Mars have extensive networks (100-1000 km2) with small size polygons (3-4m)
- Landing site of Phoenix probe in 2008 (68ºN, 234º E)
- More than 400,000 polygons in a region of 2500 x 2500 km^2

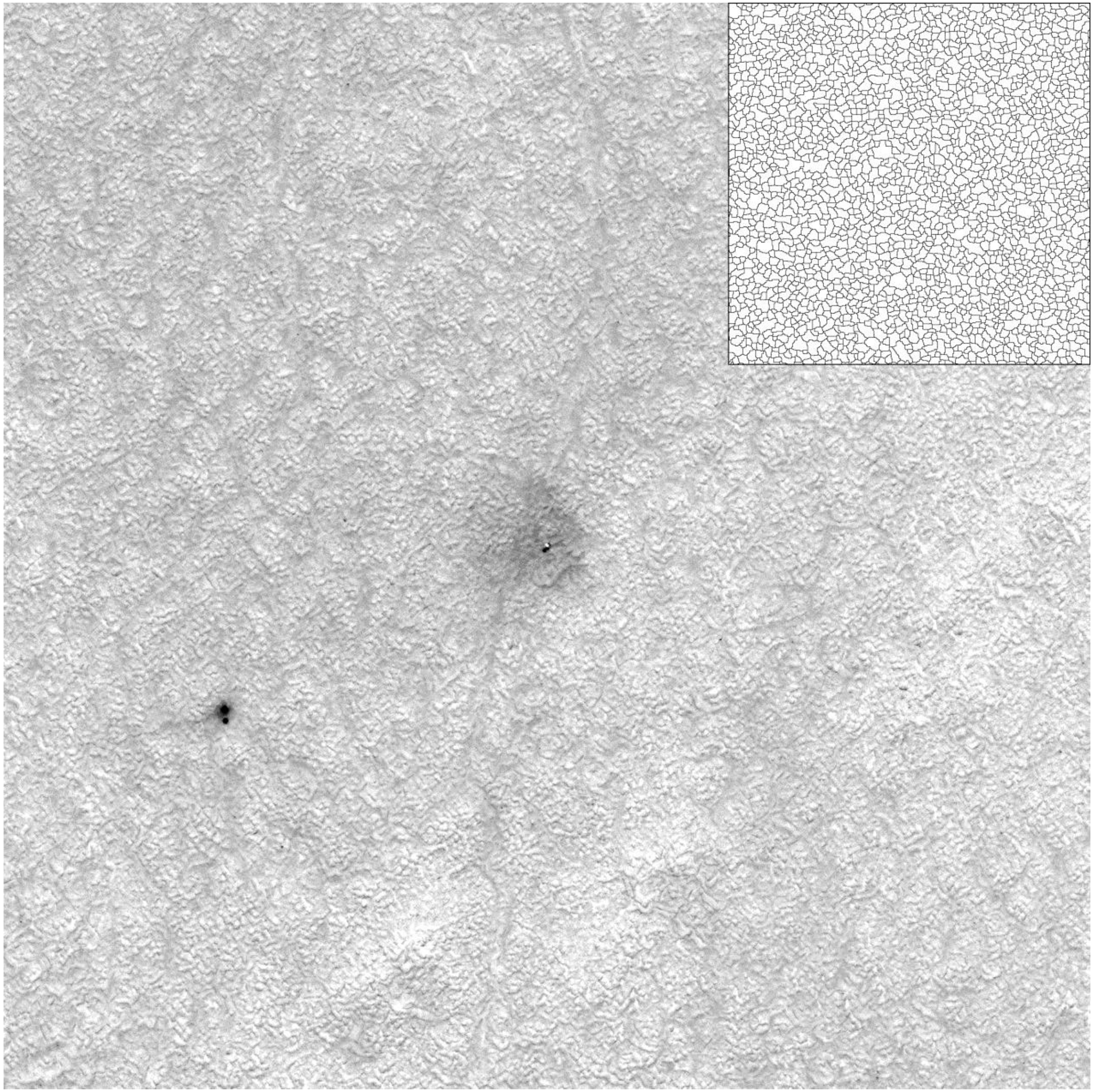

HiRISE image (0.25m/pixel)

Topologic feature extraction by morphological approaches

- Lantuéjoul (1978)

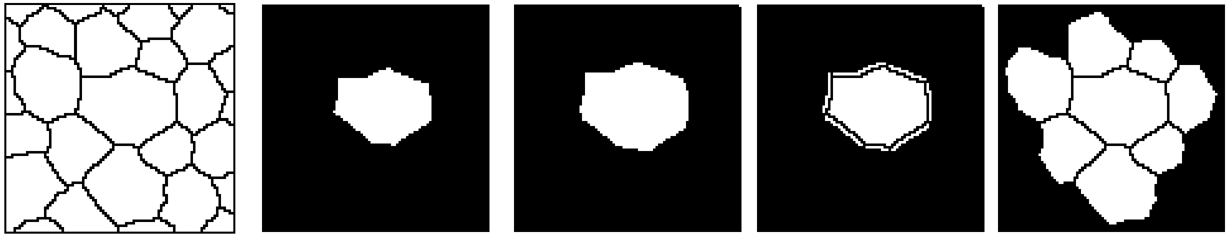

- Vincent (1989): Morphology on graphs (the detail of edges is lost)
- Pina (1996): fast morphological algorithm (only valid for trivalent networks)
- Bandeira (2008): fast morphological algortihm (difficult application in big images)

- A fast and efficient algorithm capable of dealing with every type and size of network is needed!

Fast morphological algorithm

- Based on the idea behind the 4-colour map problem: a map can be correctly painted with only 4 different colours
- Uses MM operators
- Computes i and m_i

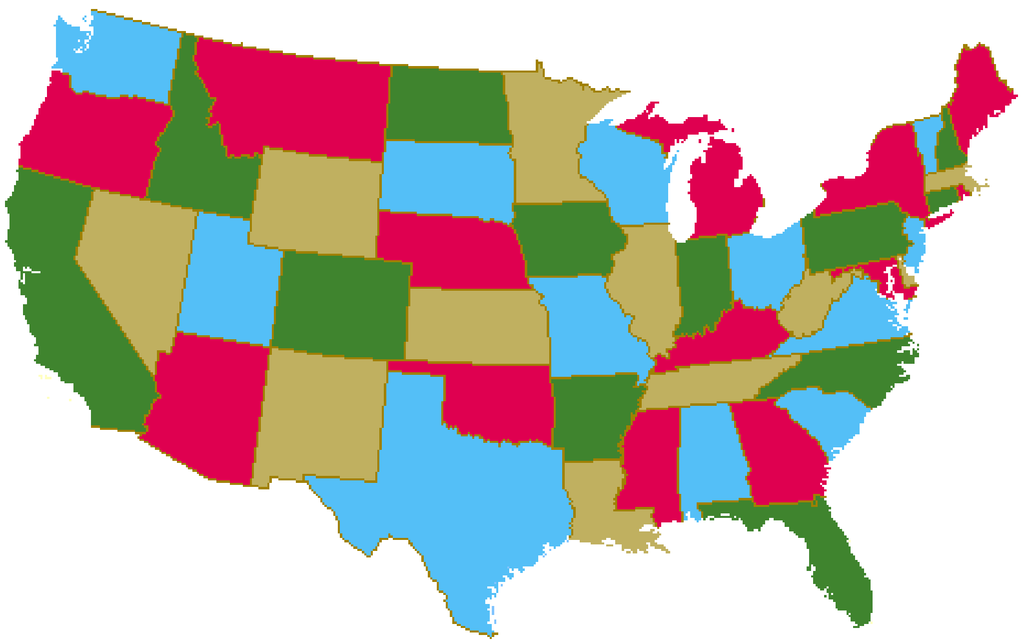

Multi-phase morphological algorithm

Phase 1 – Distribute polygons into different layers (adjacent polygons are forbidden)

1. Labelling $X = \bigcup_i x_i$

2. Distribution of polygons into *n* layers $X = B = \bigcup_{j=1,n} B(j)$

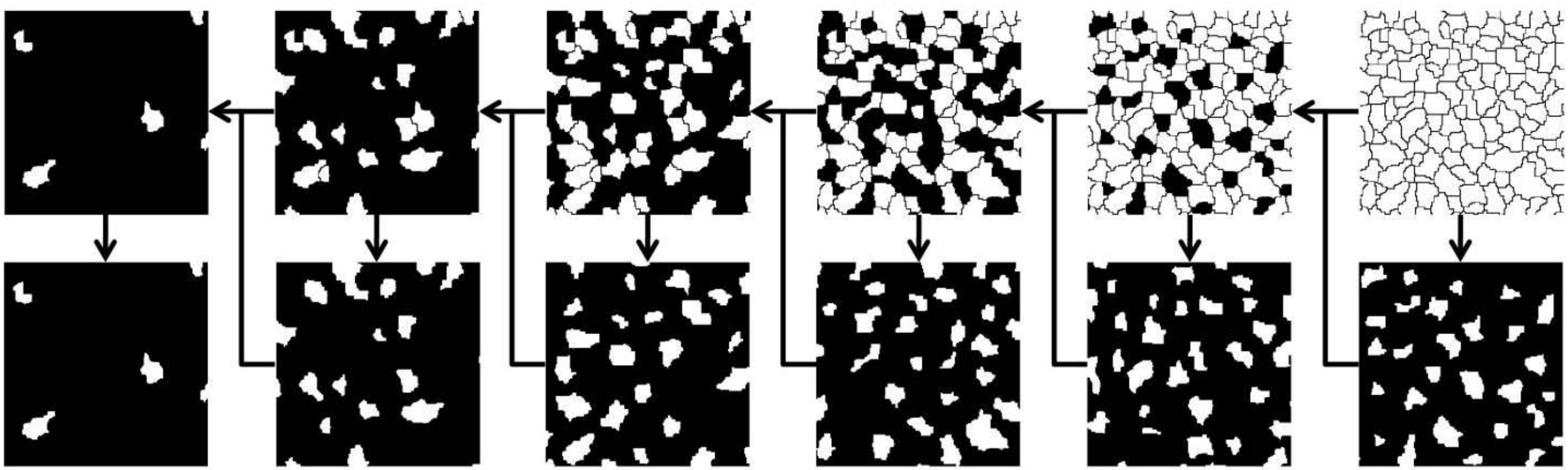

Multi-phase morphological algorithm

Phase 1 – Solve conflicts (eliminate adjacent polygons)

1. conversion of the binary layer under consideration to grey scale,

2. grey level dilation of size 2 of all polygons in the layer; if adjacent polygons exist, those with lower labels are 'invaded' by the higher values of their neighbours;

3. subtraction between (ii) and (i): non-zero pixels mark conflicting polygons;

4. binarization of (iii);

5. reconstruction of marker (iv) on the mask - initial binary layer, which indicates the conflicting polygons;

6. subtraction of the reconstructed polygons from the binary layer.

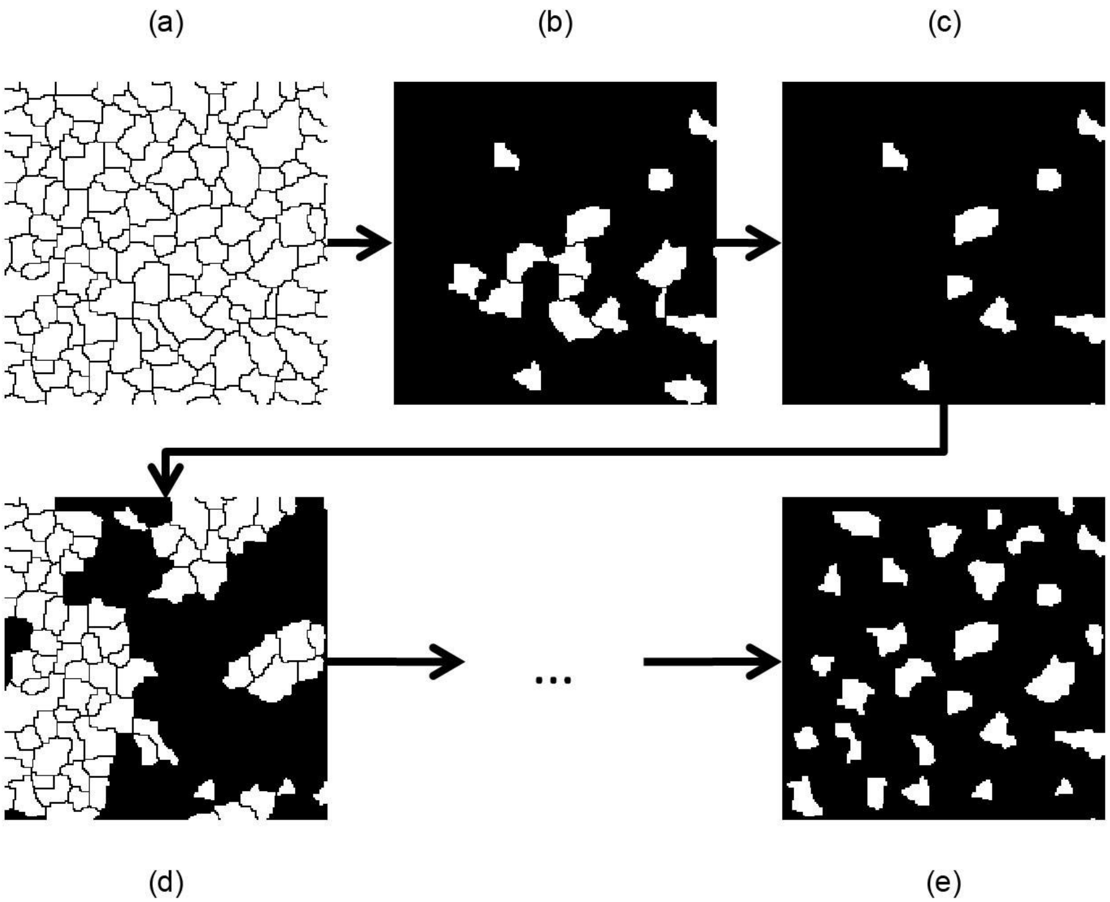

Multi-phase morphological algorithm

Phase 2 - Computation of the number of neighbours of each polygon *i*

For each layer:

1. Dilation $D(j) = \delta^{(2)}[B(j)]$
2. Intersection $S(j) = D(j) \cap X$
3. Mark neighbours $M(j) = S(j) \setminus B(j)$
4. Pruning (single point reduction) $P(j) = PRUNE^{(\infty)}(M(j)) = (M(j) OE)^{(\infty)}$
5. Counting

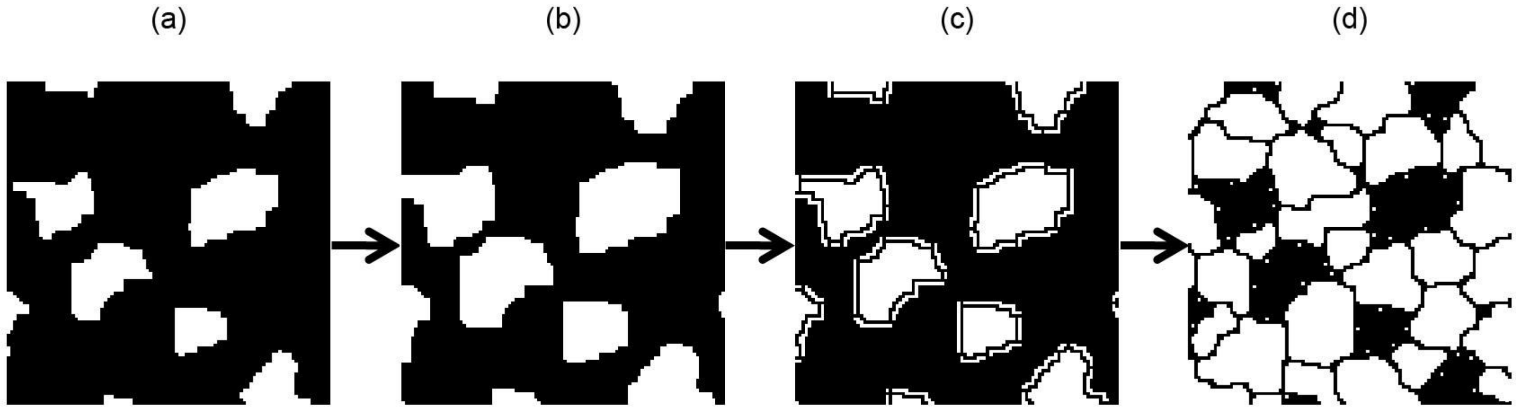

Multi-phase morphological algorithm

Phase 3 - Computation of the number of neighbours of adjacent polygons m_i

For each layer:

1. Dilation $D'(j) = \delta^{(2)}\left[f(j) \right]$
2. Multiplication $P'(j) = D'(j).P(j)$
3. Summing and dividing

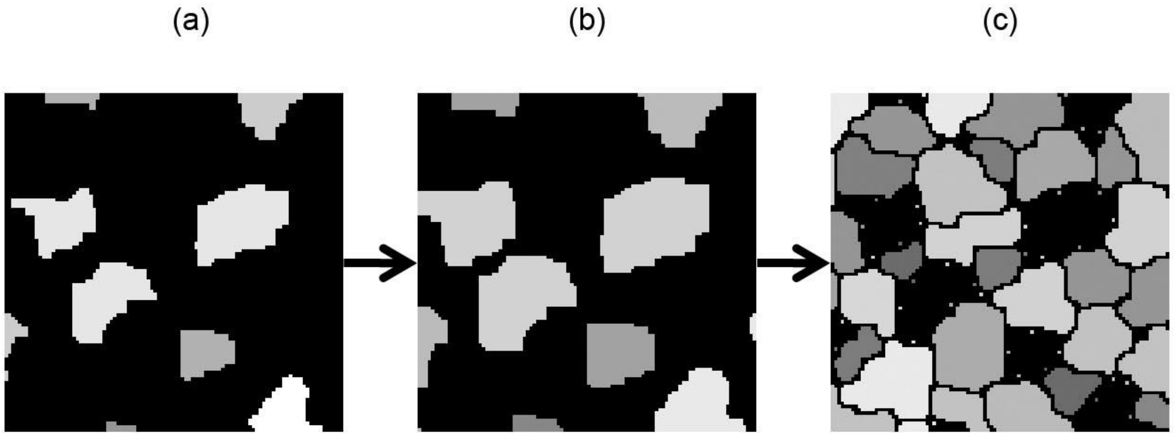

Multi-phase morphological algorithm

- Number of layers: 5-9 (achieve 4 is too expensive)
- Computational performances

  - Image 2400 x 2400 pixels, with 17,335 polygons

  - 140 times faster than Lantuéjoul’s algorithm

  - 2:30 min instead of 5:30h

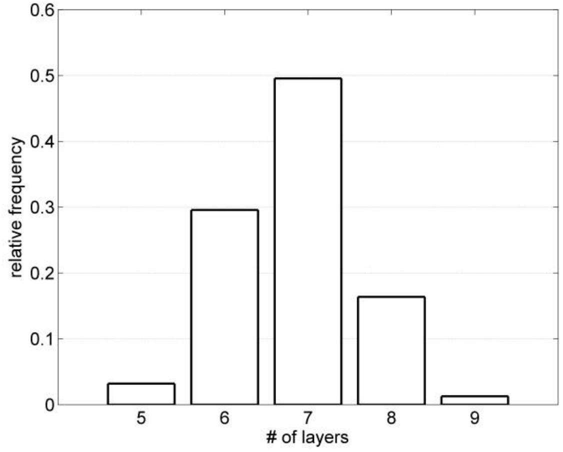

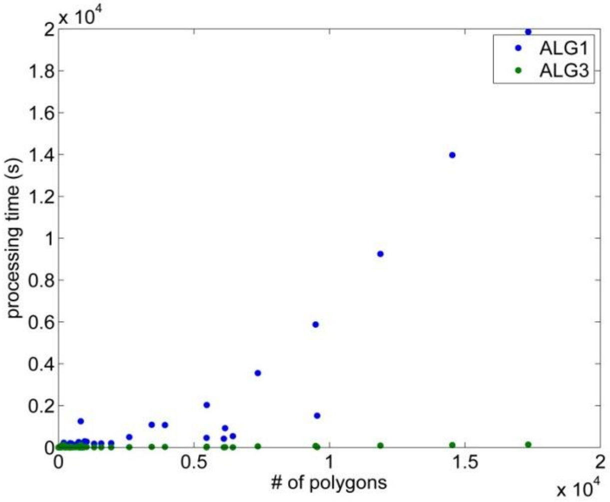

L. Bandeira, P. Pina, J. Saraiva (2010), *Pattern Recognition Letters,* 31(10): 1175-1183

Martia polygonal networks - Global Results

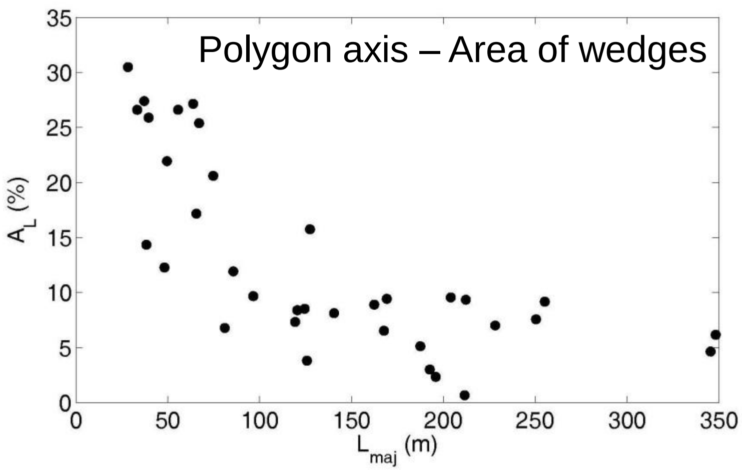

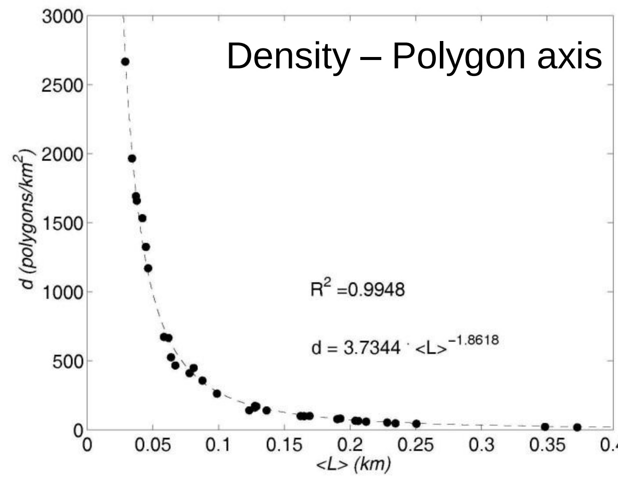

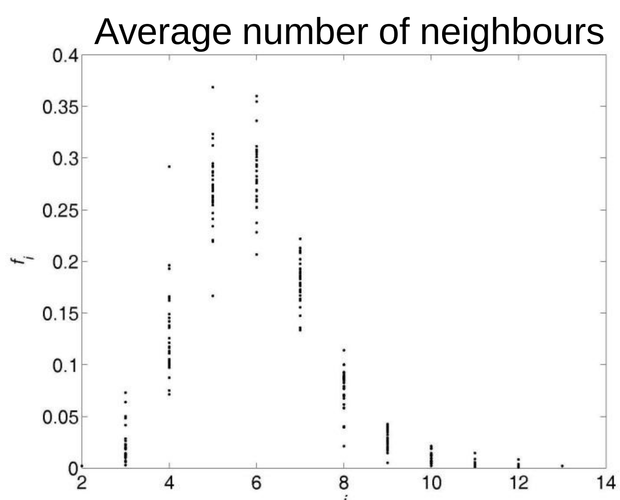

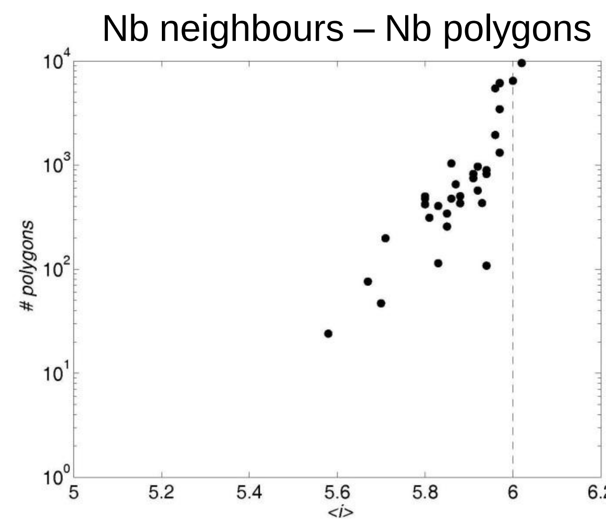

Pina P., Saraiva J., Bandeira L., Antunes J., (2008) *Planetary and Space Science*, 56(15):1919-1924

Saraiva J., Pina P., Bandeira L., Antunes J., (2009) *Philosophical Magazine Letters*, 89(3):185-193

Attempts to find clusters I

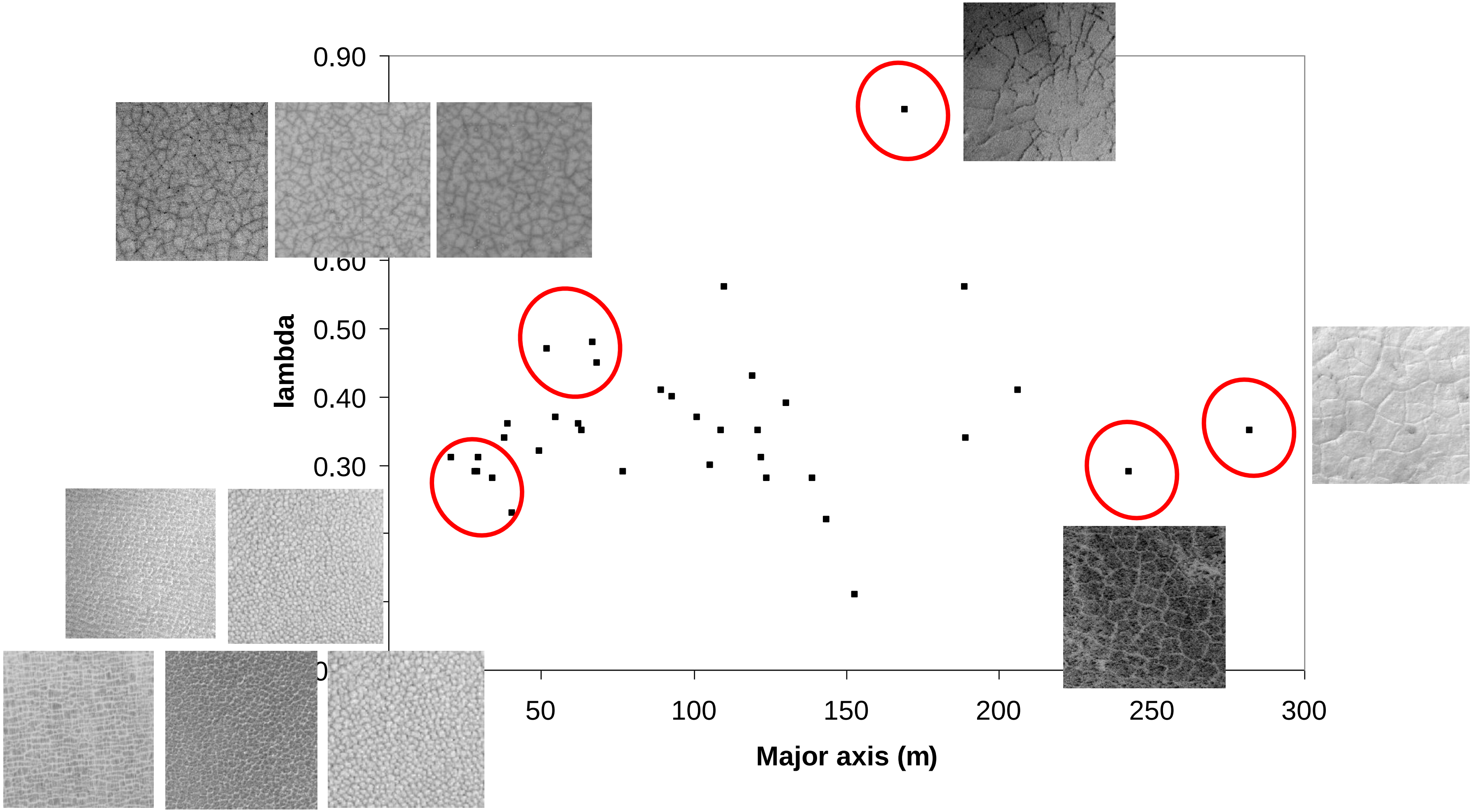

Attempts to find clusters II

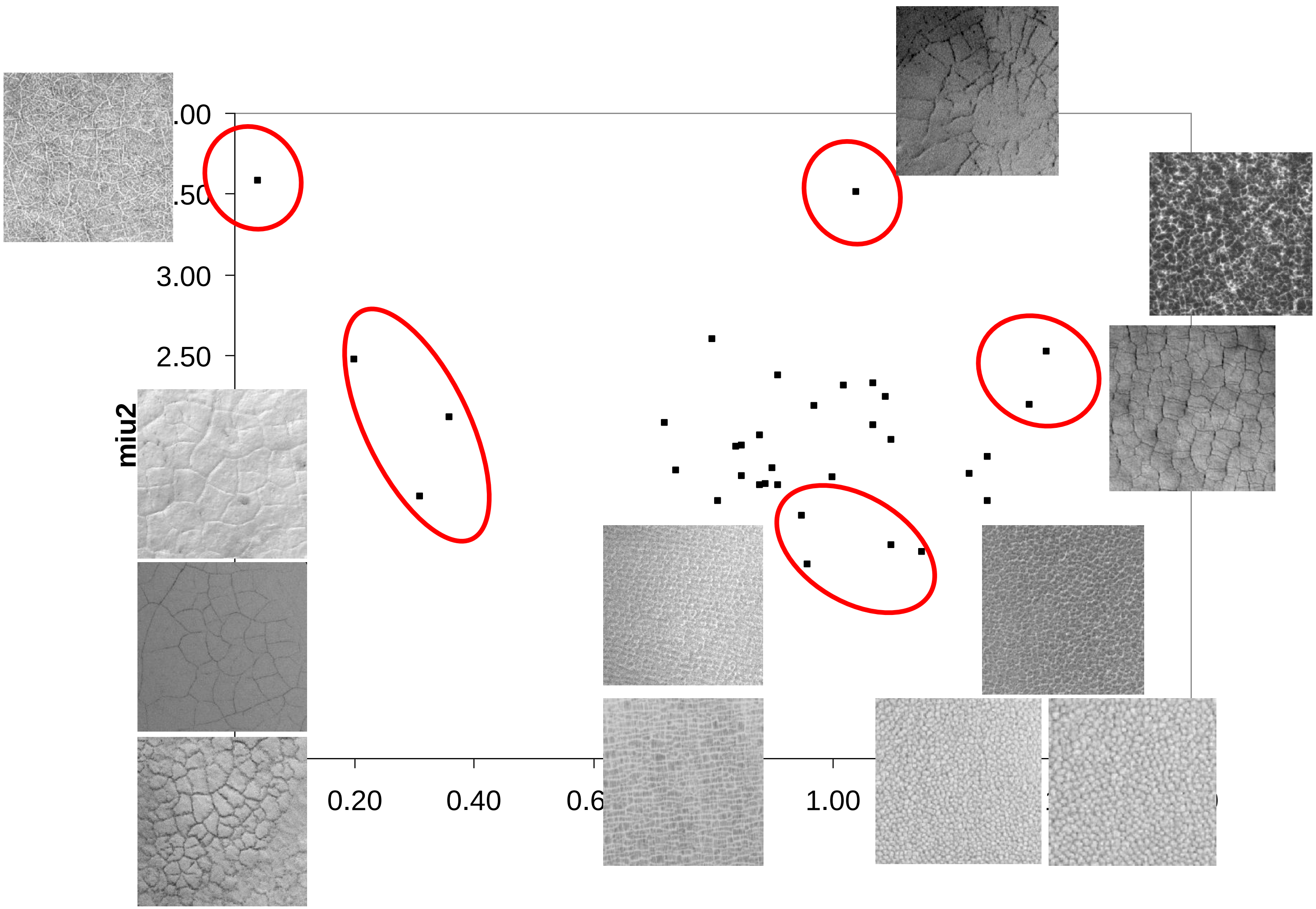

Phoenix

Polygonal patterns the landing site (~68º N, 234ºE, Martian late Spring)
- a clue to the presence of **ice in the ground**

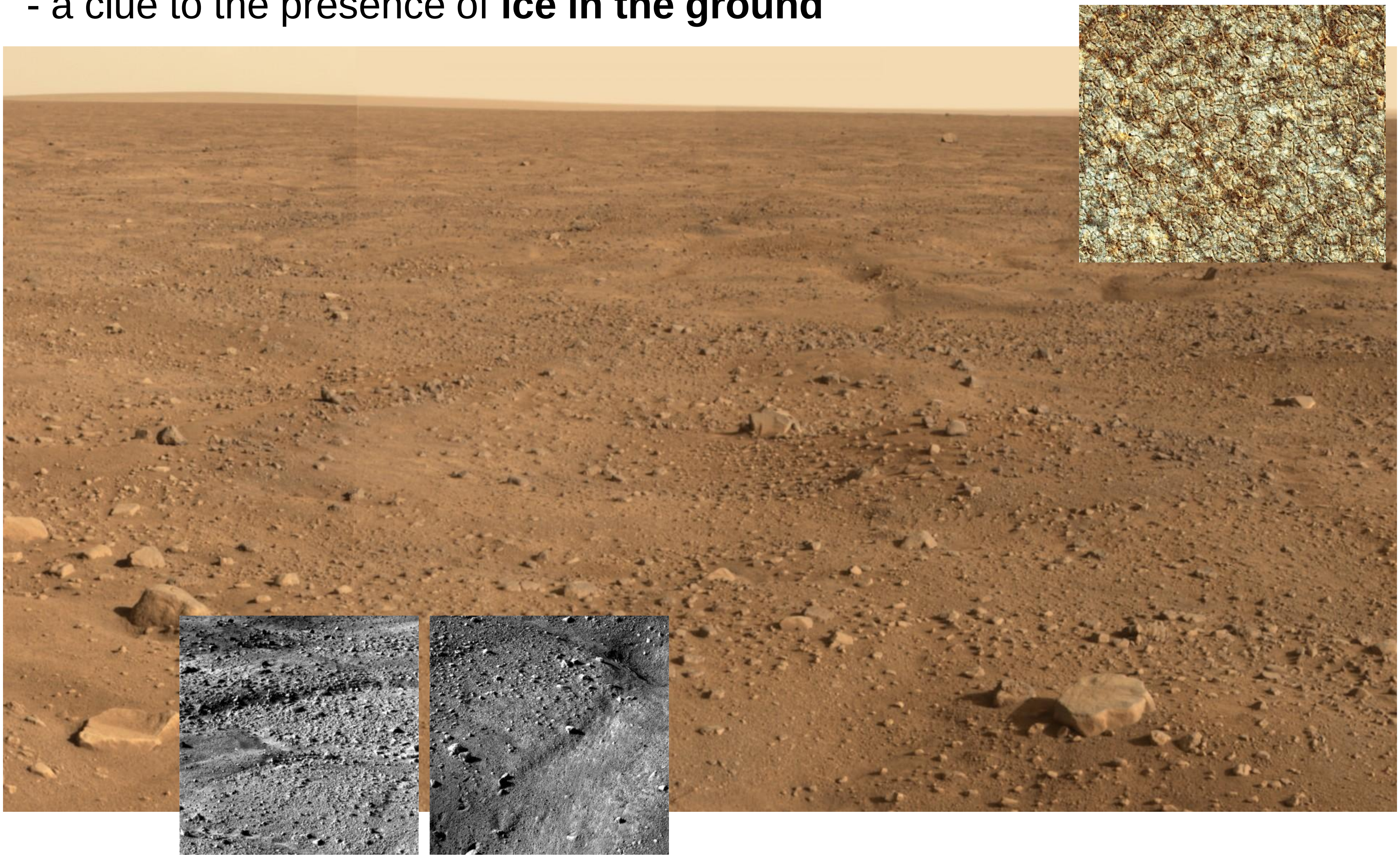

Going into the Arctic

- Studying Martian polygonal terrains with Earth analogues
- Arctic regions: Svalbard archipelago (78ºN)

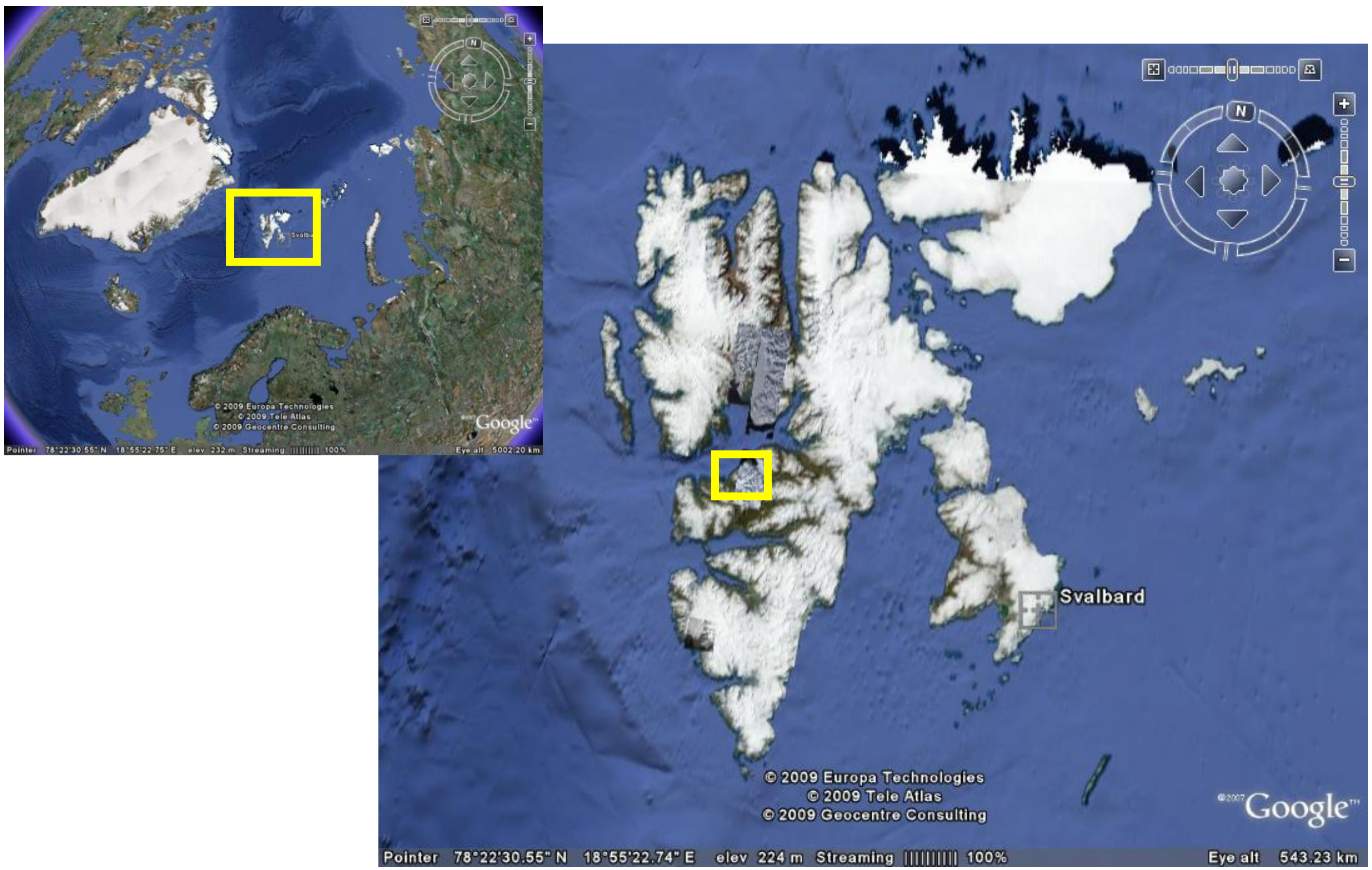

Adventdalen, Svalbard (Norway)

- Two field campaigns:

  - June 2010

  - Summer 2011

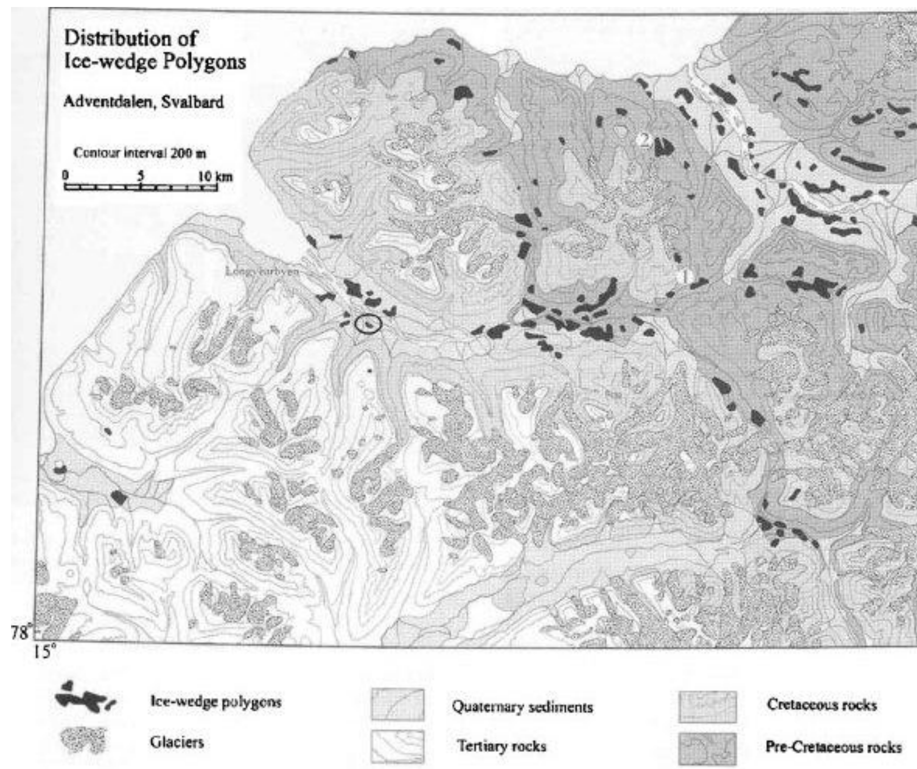

Adventdalen, Svalbard (Norway)

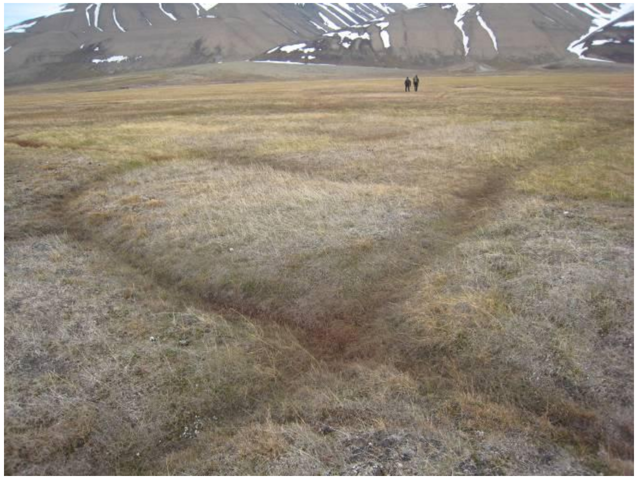




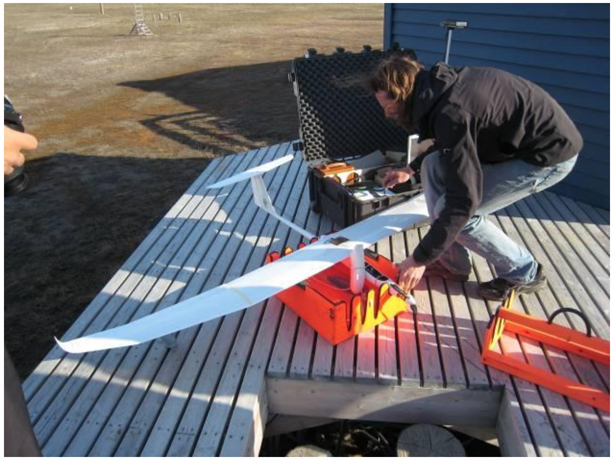

Data integration, no results yet!

Conclusion

Mathematical Morphology has been a extremely helpful tool to process planetary surface images.

Perhaps, some other solutions could be provided by other methods, but I’m sure that it would not be the same thing.

Thank you, Jean Serra!